

Global Speed Limit for Finite-Time Dynamical Phase Transition in Nonequilibrium Relaxation

Kristian Blom¹ and Aljaž Godec^{1,*}

¹*Mathematical bioPhysics group, Max Planck Institute for Multidisciplinary Sciences, Göttingen 37077, Germany*

(Dated: September 29, 2022)

Recent works unraveled an intriguing finite-time dynamical phase transition in the thermal relaxation of the mean field Curie-Weiss model. The phase transition reflects a sudden switch in the dynamics. Its existence in systems with a finite range of interaction, however, remained unclear. Employing the Bethe-Guggenheim approximation, which is exact on Bethe lattices, we here demonstrate the finite-time dynamical phase transition in nearest-neighbor Ising systems for arbitrary quenches, including those within the two-phase region. Strikingly, for any given initial condition we prove and explain the existence of non-trivial *speed limits* for the dynamical phase transition and the relaxation of magnetization, which are absent in the mean field setting. Pair correlations, which are neglected in mean field theory and trivial in the Curie-Weiss model, account for kinetic constraints due to frustrated local configurations that give rise to a global speed limit.

Despite its overwhelming importance in condensed matter physics [1, 2], our understanding of thermal relaxation kinetics is far from complete and mostly limited to systems near equilibrium [3–5] and non-equilibrium [6–8] steady states. Notable advances in understanding relaxation dynamics out of equilibrium include far-from-equilibrium fluctuation-dissipation theorems [9, 10], “frenesy” [11], anomalous relaxation a.k.a. the Mpemba effect [12–15], optimal heating and cooling [16] as well as driving [17, 18] protocols, asymmetries in heating and cooling rates [19–22], and dynamical phase transitions (i.e. the occurrence of non-analytic points in distributions of physical observables) [23–47]. Further important results on non-equilibrium relaxation are embodied in thermodynamic uncertainty relations for non-stationary systems [48–53], and so called *speed limits* [54–75].

In contrast to the well established concept of quantum speed limits [54–65] that has long been known [54], it was comparably only recently found that the evolution of classical systems is also bounded by fundamental speed limits [66–72]. Quantum and classical speed-limits impose an upper bound on the rate of change of a state of a system evolving from a given non-stationary initial state, and arise as an intrinsic dynamical property of Hilbert space [66]. Moreover, it was found that by considering the thermodynamic cost of the state change one may derive even sharper thermodynamic speed limits that bound the rate of change of a state of a system from above by the entropy production rate [68, 70, 73–75].

Recently, a surprising *finite-time dynamical phase transition* was observed in a mean field (MF) Ising system [76, 77], manifested as a finite-time singularity [78, 79] in the probability density of magnetization [76] and entropy flow per spin [77] upon a quench from any sub-critical temperature $T < T_c$ to a temperature T_q [80]. In contrast to conventional phase transitions, here time plays the role of a control parameter inducing an abrupt change of the

typical dynamics [76, 77]. The sudden transition from a Gibbsian to a non-Gibbsian probability density occurs for *all* quenches from sub-critical temperatures $T < T_c$, whereby the initial location of the singularity depends on T and T_q [79]. Upon quenches from super-critical temperatures $T > T_c$ the probability density remains Gibbsian forever [79], but the dynamics is non-ergodic [81].

Notwithstanding the detailed results on the non-Gibbsian transition in the MF setting, it remains unknown if and in what form this novel dynamical phase transition exists in systems with a finite range of interactions. Moreover, since speed limits bound from below the time of reaching a final state from a given initial state, the following intriguing questions arise: *What happens with the speed limit in the finite-time dynamical phase transition, where the dynamics experiences an abrupt change? Is there a global speed limit to reaching the critical time?*

To shed light on these questions we here present analytical results on non-equilibrium relaxation of nearest-neighbor Ising systems on the Bethe-Guggenheim (BG) level [82, 83], which accounts for nearest-neighbor pair correlations and is exact for the nearest-neighbor Ising model on the Bethe lattice. Our results confirm, for the first time, the existence of the finite-time dynamical phase transition in finite-range Ising systems. Strikingly, we derive explicit *global* speed limits to both, the critical time and relaxation time, which are absent in the MF setting. Notably, the speed limit is set by an antiferromagnetic interaction and is faster than the dynamics of a non-interacting system. Accounting for kinetically unfavorable local spin configurations, pair correlations, which are neglected in MF theory, impose a global speed limit in the non-Gibbsian dynamical phase transition.

Fundamentals.—The Hamiltonian of nearest-neighbor interacting Ising spins $\sigma_i = \pm 1$, $i = \{1, \dots, N\}$ reads

$$H(\boldsymbol{\sigma}, J) = -J \sum_{\langle ij \rangle} \sigma_i \sigma_j, \quad (1)$$

with J denoting the ferromagnetic ($J > 0$) or antiferromagnetic ($J < 0$) coupling and $\langle ij \rangle$ the sum over

* agodec@mpinat.mpg.de

nearest neighbor spin pairs. The spins are placed on a Bethe lattice with coordination number $\bar{z} \in \mathbb{N}^+$. Three examples of Bethe lattices are shown in Fig. 1a. Let $m(\boldsymbol{\sigma}) \equiv N^{-1} \sum_{i=1}^N \sigma_i$ be the magnetization per spin for a given configuration $\boldsymbol{\sigma} = (\sigma_1, \dots, \sigma_N)$. The equilibrium free energy density in the thermodynamic limit is defined as $f(m, J) = \lim_{N \rightarrow \infty}^{m=\text{const.}} [N^{-1} \ln(\mathcal{Z}_m(J))]$, where $\mathcal{Z}_k(J) \equiv \sum_{\boldsymbol{\sigma}} \exp(-H(\boldsymbol{\sigma}, J)/k_B T) \mathbb{1}_{m(\boldsymbol{\sigma}), k}$ is the fixed-magnetization partition function with indicator function $\mathbb{1}_{a,b}$ being 1 when $a = b$ and 0 otherwise. Within BG theory, the free energy density in units of $k_B T$, $\tilde{f}_{\text{BG}} \equiv f_{\text{BG}}/k_B T$, reads (exactly for Bethe lattices) [82–84]

$$\tilde{f}_{\text{BG}}(m, \tilde{J}) = 2\bar{z}\tilde{J}(\zeta(m) - 1/4) + (1 - \bar{z})[\Xi(m) + \Xi(-m)] + \frac{\bar{z}}{2} \sum_{\eta=\pm} [\Xi(\eta m - \zeta(m)) + \Xi(\zeta(m) - 1)], \quad (2)$$

where $\Xi(m) \equiv (1/2 + m/2) \ln(1/2 + m/2)$, $\tilde{J} \equiv J/k_B T$, and

$$\zeta(m) \equiv \frac{1 - m^2}{1 + [m^2 + \exp(4\tilde{J})(1 - m^2)]^{1/2}}. \quad (3)$$

The MF counterpart is recovered by applying the transformation $\zeta(m) \rightarrow (1 - m^2)/2$, or equivalently to setting $\tilde{J} = 0$ in Eq. (3) [85]. The BG critical temperature below which $\tilde{f}_{\text{BG}}(m, \tilde{J})$ develops two degenerate minima reads $\tilde{J}_c^{\text{BG}} \equiv \ln(\bar{z}/(\bar{z} - 2))/2$, and correctly diverges in dimension one with $\bar{z} = 2$, where no phase transition occurs.

We now introduce stochastic dynamics for changes of the magnetization within the *local equilibrium* approximation [86, 87], which is highly accurate in the thermodynamic limit [84]. Let $W^\pm(M, \tilde{J})$ denote the transition rate to change the total magnetization from $M \equiv Nm \rightarrow M \pm 2$ by a single-spin flip. Following [86, 87] we define, in the thermodynamic limit, an intensive transition rate $w^\pm(m, \tilde{J}) \equiv \lim_{N \rightarrow \infty}^{m=\text{const.}} [W^\pm(Nm, \tilde{J})/N]$, which on the BG-local equilibrium level reads

$$w_{\text{BG}}^\pm(m, \tilde{J}) = \frac{1 \mp m}{2\tau} \left(e^{-\tilde{J}} + \frac{2\zeta(m) \sinh(\tilde{J})}{1 \mp m} \right)^{\bar{z}}, \quad (4)$$

τ being an intrinsic time-scale of infinitesimal changes of magnetization $m \rightarrow m + dm$ [88]. The transition rates obey the parity symmetry $w_{\text{BG}}^\pm(m, \tilde{J}) = w_{\text{BG}}^\mp(-m, \tilde{J})$ and detailed balance w.r.t. the free energy density, $w_{\text{BG}}^\pm(m, \tilde{J})/w_{\text{BG}}^\mp(m, \tilde{J}) = \exp(-2\partial_m \tilde{f}_{\text{BG}}(m, \tilde{J}))$. In the weak coupling (or high temperature) limit we recover MF transition rates $\lim_{\tilde{J} \rightarrow 0} w_{\text{BG}}^\pm(m, \tilde{J}) = w_{\text{MF}}^\pm(m, \tilde{J}) + \mathcal{O}(\tilde{J}^2)$ reported in [76]. A comparison of BG and MF transition rates for $(\bar{z}, \tilde{J}) = (4, 0.5)$ is shown in Fig. 1b.

Let $P_N(m, \tilde{J}, t)$ be the probability density of m at time t evolving according to the incoming and outgoing local fluxes $\partial_t P_N(m, \tilde{J}, t) = j^+(m, t) - j^-(m, t)$. Let $V(m, \tilde{J}, t) \equiv -\lim_{N \rightarrow \infty} N^{-1} \ln P_N(m, \tilde{J}, t)$ denote the time-dependent large-deviation rate function. At equilibrium the rate function is given by $V_{\text{eq}}(m, \tilde{J}) \equiv \tilde{f}(m, \tilde{J}) -$

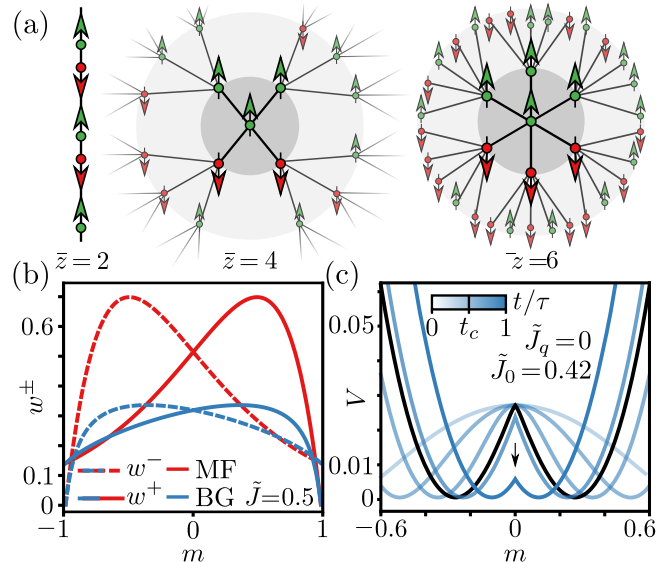


FIG. 1. (a) Examples of Bethe lattices. In (b)-(c) we consider a Bethe lattice with $\bar{z}=4$. (b) Forward (solid lines) and backward (dashed lines) rates w^\pm within the BG (blue; see Eq. (4)) and MF approximation (red; see [76]). (c) Temporal evolution of $V(m, \tilde{J}, t)$ upon a quench into the one-phase domain. Time increases from light to dark blue lines. At the critical time t_c (black line) a cusp emerges at $m = 0$.

$\tilde{f}(\bar{m}, \tilde{J})$ with $\bar{m}(\tilde{J}) \equiv \arg \min_m \tilde{f}(m, \tilde{J})$ denoting the location of free energy minima. Out of equilibrium $V(m, \tilde{J}, t)$ obeys a Hamilton-Jacobi equation [76, 89, 90]

$$\partial_t V(m, \tilde{J}, t) + \mathcal{H}(m, \partial_m V(m, \tilde{J}, t)) = 0, \quad (5)$$

with the Hamiltonian given by

$$\mathcal{H}(q, p) = w^+(q, \tilde{J})(e^{2p} - 1) + w^-(q, \tilde{J})(e^{-2p} - 1). \quad (6)$$

Eq. (5) can be derived directly from the master equation for $P_N(m, \tilde{J}, t)$ as the instanton solution in the thermodynamic limit. We are interested in the evolution of $V(m, \tilde{J}, t)$ upon a quench $\tilde{J} \rightarrow \tilde{J}_q < \tilde{J}$, where \tilde{J}_q may be positive or negative. Experimentally quenches to negative \tilde{J}_q may be achieved, e.g. by ultrafast optical switching ferro-antiferromagnetic materials [91] or by spin-population inversion in metals by radio-frequency irradiation [92] yielding negative spin temperatures [93]. Note that quenches beyond the Néel point (i.e. the antiferromagnetic critical point) push the system across the antiferromagnetic transition, which m does not detect [94–97]. In fact, quenching from the antiferromagnetic two-phase region and replacing m with the staggered magnetization [94–97] yields mirror-symmetric results (see [98]).

Dynamical phase transition.—We throughout assume that the system is initially prepared at equilibrium in the two-phase regime $\tilde{J}_0 > \tilde{J}_c^{\text{BG}}$ (i.e. below the Curie temperature), and thus $V_{\text{BG}}(m, \tilde{J}, 0) = \tilde{f}_{\text{BG}}(m, \tilde{J}_0) - \tilde{f}_{\text{BG}}(\bar{m}, \tilde{J}_0)$. At $t = 0$ we apply an instantaneous quench $\tilde{J}_q < \tilde{J}_0$ by changing T or J , which pushes the system out of equilibrium. The rate function $V_{\text{BG}}(m, \tilde{J}, t > 0)$ thereupon evolves according to Eq. (5), which we solve nu-

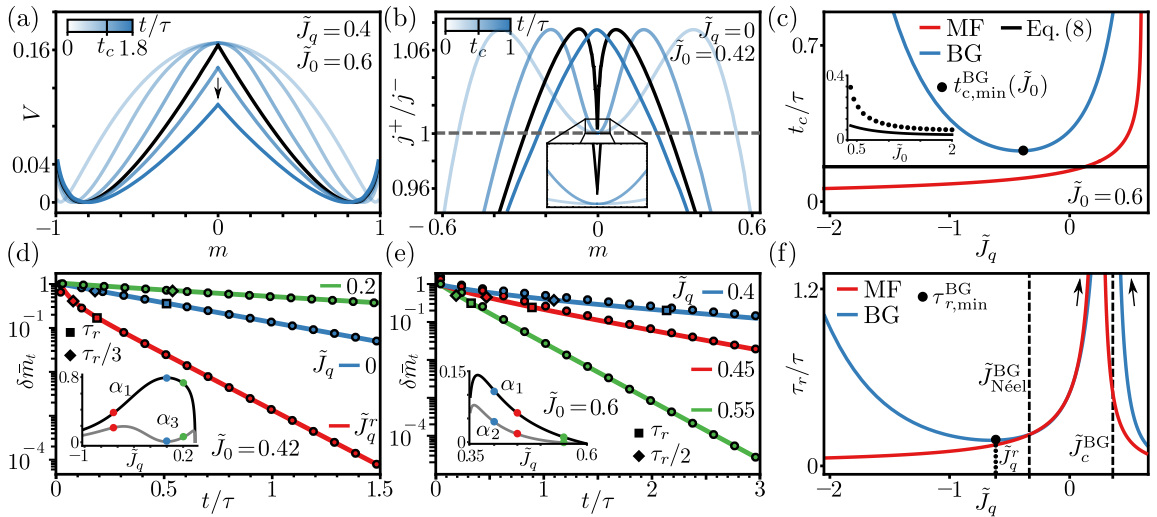


FIG. 2. (a) Temporal evolution of the BG rate function $V(m, \tilde{J}_q, t)$ upon a quench into the two-phase domain. (b) Temporal evolution of the probability-flux ratio $j^+(m, t)/j^-(m, t)$ after a quench into the one-phase regime. At the critical time t_c (black line) the ratio discontinuously jumps to a value above 1 at $m = 0$. Inset: Enlargement around $m = 0$. (c) BG (blue) and MF (red) critical time t_c/τ as a function of \tilde{J}_q . The BG critical time attains a global minimum $t_{c,\min}^{\text{BG}}$ (black dot) for an antiferromagnetic quench, bounded from below by Eq. (8); Inset: $t_{c,\min}^{\text{BG}}$ (black dots) and Eq. (8) (black line) as a function of \tilde{J}_0 . (d-e) Relaxation of excess mean magnetization $\delta\tilde{m}_t = (\tilde{m}_t - \tilde{m}_\infty)/(\tilde{m}_0 - \tilde{m}_\infty)$ upon a quench in the one- (d) and two-phase (e) domain. Dots depict the first two nonzero terms of the analytical power series solution, lines are numerical solutions of the differential equation. Squares/diamonds denote the first τ_r and second ($\tau_r/3$ in d and $\tau_r/2$ in e) relaxation time-scales, respectively. Inset: First two nonzero prefactors of the power series. (f) BG (blue) and MF (red) relaxation time τ_r/τ as a function of quench temperature \tilde{J}_q . τ_r^{BG} has a local minimum at \tilde{J}_q^{BG} (see Eq. (9)). In all panels $\bar{z} = 4$.

merically (see Fig. 1d and 2a for quenches $\tilde{J}_q \leq \tilde{J}_c^{\text{BG}}$ and $\tilde{J}_q \geq \tilde{J}_c^{\text{BG}}$, respectively). As $V_{\text{BG}}(m, \tilde{J}, t)$ relaxes towards the new equilibrium at \tilde{J}_q , there is a defined moment $t_c^{\text{BG}}(\tilde{J}_0, \tilde{J}_q)$ —the critical time—where $V_{\text{BG}}(m, \tilde{J}, t)$ abruptly develops a cusp (black line in Fig. 1c and 2a) and becomes non-Gibbsian. The phenomenon was coined finite-time dynamical phase transition [76, 78, 79] and is hereby confirmed in nearest-neighbor Ising systems.

The reflection symmetry around $m=0$ and local rates w_{BG}^+ and w_{BG}^- that are strictly increasing and decreasing, respectively, in an interval around $m = 0$ (see Fig. 1b), ensure that the forward, $j^+(m, t)$, and backward, $j^-(m, t)$, probability fluxes remain perfectly balanced in a region around $m = 0$ during a transient period after the quench (see Fig. 2b). As a result, $P_N(m \approx 0, \tilde{J}, t)$ is transiently “locked” in the initial state (see Fig. 1c and Fig. 2a). “Fronts” of net flux towards $m = 0$ gradually develop on each side and drift towards the center (Fig. 2b). Once the fronts collide, the dynamical phase transition takes place as an instability, in which the flux ratio $j^+(0, t)/j^-(0, t)$ discontinuously jumps to a value larger than 1 (inset of 2b). At the transition the dynamics switches from *confined in the wells* to *exploring the free energy barrier*, i.e. between the formation of defects in ordered domains to their (partial) melting.

The fact that the cusp appears upon quenches within the two-phase regime, $\tilde{J}_c^{\text{BG}} \leq \tilde{J}_q < \tilde{J}_0$ (see Fig. 2a), implies that the dynamical phase transition does not re-

quire a change in geometry from a double- to a single-well potential. Moreover, we show (see [98]) that the initial location of the cusp undergoes a symmetry-breaking transition below the threshold temperature $\tilde{J}_0 > \tilde{J}_0^{\text{SB}}(\tilde{J}_q)$ whereupon it moves from the center $m = 0$. For infinite temperature quenches the symmetry-breaking temperature converges to $\tilde{J}_{0,\text{BG}}^{\text{SB}}(0) = \ln([z+1]/[z-2])/2$, which in the MF setting simplifies to $\lim_{z \rightarrow \infty} \tilde{J}_{0,\text{BG}}^{\text{SB}}(0) = 3/(2z) + \mathcal{O}(1/z^2)$ [78, 79].

Critical time.—We now determine the critical time t_c , i.e. the first instance a cusp appears at $m = 0$. The critical time can be determined from the curvature [76] or slope [78, 79] at $m = 0$ and reads (see derivation in [98])

$$t_c(\tilde{J}_0, \tilde{J}_q) = \frac{\ln(1 - \tilde{f}''(0, \tilde{J}_q)/\tilde{f}''(0, \tilde{J}_0))}{8w^\pm(0, \tilde{J}_q)\tilde{f}''(0, \tilde{J}_q)}, \quad (7)$$

where $\tilde{f}''(0, \tilde{J}) \equiv d^2\tilde{f}(m, \tilde{J})/dm^2|_{m=0}$ and all appearing quantities are given in Eqs. (2)-(4). Using the MF free energy density and transition rates in Eq. (7) we recover the results derived in [76, 78, 79]. The BG (blue) and MF (red) critical times as a function of \tilde{J}_q are shown in Fig. 2c for $(\bar{z}, \tilde{J}_0) = (4, 0.6)$ and display starkly dissimilar behavior. In particular, the BG critical time displays a global minimum—a *global speed limit*—that is absent in the MF setting. This implies a dominant role of local spin configurations, which are accounted for in the BG theory but ignored in MF theory.

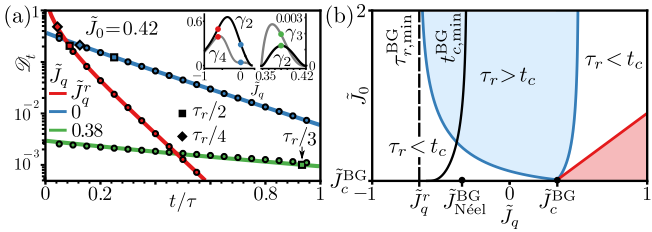


FIG. 3. (a) Temporal evolution of the relative entropy per spin \mathcal{S}_t upon a quench into the one-phase (red and blue) and two-phase regime (green). At \tilde{J}_q^r (red) the relative entropy relaxes the fastest. Dots depict analytical results obtained with the first two nonzero terms in Eq. (10). Lines correspond to numerical results. Squares/diamonds denote the first $\tau_r/2$ and second $\tau_r/4 - \tau_r/3$ relaxation time-scales, respectively. Inset: First two nonzero prefactors which enter Eq. (10). (b) Dynamical phase diagram for t_c^{BG} and τ_r^{BG} . The red area is forbidden since $\tilde{J}_0 > \tilde{J}_q$. Dashed/solid black lines denote the fastest relaxation and critical time. Both panels correspond to $\bar{z} = 4$.

Antiferromagnetic quenches bound the critical time.—

The stationary points of Eq. (7) cannot be determined analytically. To confirm that the speed limit indeed exists we instead prove a lower bound on Eq. (7). The critical time $t_c(\tilde{J}_0, \tilde{J}_q)$ is monotonically increasing with \tilde{J}_q for $\tilde{J}_c^{\text{BG}} \leq \tilde{J}_q < \tilde{J}_0$ (see proof in [98]). Thus, the critical time for quenches within the two-phase regime is bounded from below by $\tilde{J}_q = \tilde{J}_c^{\text{BG}}$, where $t_c^{\text{BG}}(\tilde{J}_0, \tilde{J}_c^{\text{BG}}) = -(\bar{z} - 1)^{\bar{z}} / (4(\bar{z}^2 - 2\bar{z})^{\bar{z}/2} \tilde{f}''(0, \tilde{J}_0))$.

For quenches beyond the critical point, i.e. $\tilde{J}_q < \tilde{J}_c^{\text{BG}}$, we have $-\tilde{f}_{\text{BG}}''(0, \tilde{J}_q) / \tilde{f}_{\text{BG}}''(0, \tilde{J}_0) > 0$ and we can apply the inequality $\ln(1+x) > 2x/(2+x)$ for $x > 0$ [99] to the numerator of Eq. (7). Minimizing the result with respect to \tilde{J}_q then yields a speed limit on the critical time

$$t_{c,\min}^{\text{BG}}(\tilde{J}_0) > \frac{\cosh^{\bar{z}}(\ln[e^{2\tilde{J}_c^{\text{BG}}} (e^{-2\tilde{J}_0} + 2/\bar{z} + \Delta_{\bar{z}}(\tilde{J}_0))]/2)}{\bar{z} - e^{2\tilde{J}_c^{\text{BG}}}[(\bar{z}-4)e^{-2\tilde{J}_0} - 4/\bar{z} - \bar{z}\Delta_{\bar{z}}(\tilde{J}_0)]}, \quad (8)$$

where $\Delta_{\bar{z}}(\tilde{J}_0) \equiv [8/\bar{z}^2 + e^{-4\tilde{J}_0} + (1-4/\bar{z})(1-2e^{-2\tilde{J}_0})]^{\frac{1}{2}}$. The bound becomes tighter with increasing \tilde{J}_0 (see inset Fig. 2c) and \bar{z} (see [98]), and for $\tilde{J}_0 \rightarrow \infty$ attains a minimum value which reads $1/8$ for $\bar{z} = 4$ (see [98] for the general result). The bound (8) is by construction smaller than $t_c^{\text{BG}}(\tilde{J}_0, \tilde{J}_c^{\text{BG}})$ and therefore also bounds quenches within the two-phase domain. Notably, the BG critical time attains a minimum for an antiferromagnetic quench $\tilde{J}_q < \tilde{J}_{\text{Néel}}^{\text{BG}} < 0$ (see black point in Fig. 2c), which lies below the Néel point $\tilde{J}_{\text{Néel}}^{\text{BG}} = -\tilde{J}_c^{\text{BG}}$ [95, 96].

Antiferromagnetic speed limit for relaxation.—

Interestingly, we now show that an antiferromagnetic speed limit also exists in the relaxation of the mean magnetization $\langle m_t \rangle \equiv \int_{-1}^1 m P_N(m, \tilde{J}, t) dm$. In the thermodynamic limit $\langle m_t \rangle$ is dominated by $\tilde{m}_t \equiv \arg \min_m V(m, t, \tilde{J}_q)$ [100], where $\pm \tilde{m}_t$ evolve according to $\frac{d}{dt} \tilde{m}_t(\tilde{J}_0, \tilde{J}_q) = 2(w^+(\tilde{m}_t, \tilde{J}_q) - w^-(\tilde{m}_t, \tilde{J}_q))$, with initial condition $\tilde{m}_0 = \arg \min_m \tilde{f}(m, \tilde{J}_0)$ [88].

Using the Lagrange inversion theorem we obtain an explicit power-series solution $\tilde{m}_t(\tilde{J}_0, \tilde{J}_q) = \sum_{k=0}^{\infty} \alpha_k(\tilde{J}_0, \tilde{J}_q) e^{-kt/\tau_r(\tilde{J}_q)}$ (see [98] for details) with relaxation rate $1/\tau_r(\tilde{J}_q) \equiv 4w^{\pm}(\tilde{m}_{\infty}, \tilde{J}_q) \tilde{f}'''(\tilde{m}_{\infty}, \tilde{J}_q)$. The prefactors α_k are given explicitly in [98]. In Fig. 2d-e we show the relaxation of the relative excess magnetization $\delta \tilde{m}_t \equiv (\tilde{m}_t - m_{\infty}) / (m_0 - m_{\infty})$ for quenches into the one-phase (panel d) and two-phase (panel e) domain, based on a numerical solution (lines) and by retaining only the first two terms in the power-series (dots).

For quenches beyond the critical point $\tilde{J}_q < \tilde{J}_c^{\text{BG}}$ the relaxation rate depends non-monotonically on \tilde{J}_q (compare red and green lines in Fig. 2d), which is explicitly elaborated in Fig. 2f. Similarly to the critical time we find a speed limit, i.e. $\tau_r^{\text{BG}}(\tilde{J}_q)$ is minimal at an antiferromagnetic quench \tilde{J}_q^r below the Néel point

$$\tilde{J}_q^r \equiv \arg \min_{\tilde{J}_q} \tau_r^{\text{BG}}(\tilde{J}_q) = \frac{1}{2} \ln \left(\frac{\bar{z} - 2\sqrt{\bar{z}-1}}{\bar{z}-2} \right) < \tilde{J}_{\text{Néel}}^{\text{BG}}. \quad (9)$$

For $\bar{z} = 4$ this gives $\tilde{J}_q^r \approx -0.65874$ as indicated in Fig. 2f with the black dotted line. The antiferromagnetic speed limit $\tau_r(\tilde{J}_q^r)$ is the result of a trade-off between an antiferromagnetic interaction deterministically biasing m towards smaller values on the one hand, and growing kinetic constraints on energetically accessible local configurations on the other hand. When $\tilde{J}_q > \tilde{J}_c^{\text{BG}}$, i.e. for quenches within the two-phase regime, there is no speed limit and τ_r decreases monotonically with \tilde{J}_q towards zero because all quenches become vanishingly small, $\tilde{m}_0 - \tilde{m}_{\infty} \rightarrow 0$.

Asymptotic measure equivalence.—Despite the presence of a cusp in the rate function for all $t > t_c$ (see proof in [98]) we now show that $P_{N \rightarrow \infty}(m, \tilde{J}, t)$ becomes measure equivalent [101, 102] to the equilibrium Gibbs measure exponentially fast. We quantify the distance between the two measures via the instantaneous excess free energy density \mathcal{D}_t [19, 103–108] defined as the relative entropy per spin in the thermodynamic limit, $\mathcal{D}_t \equiv \lim_{N \rightarrow \infty} \frac{1}{N} D[P_N(m, \tilde{J}, t) | | P_N^{\text{eq}}(m, \tilde{J})]$, or explicitly

$$\begin{aligned} \mathcal{D}_t &= \lim_{N \rightarrow \infty} \int_{-1}^1 e^{-NV(m, \tilde{J}_q, t)} [V_{\text{eq}}(m, \tilde{J}_q) - V(m, \tilde{J}_q, t)] dm \\ &\simeq \sum_{k=2}^{\infty} \gamma_k(\tilde{J}_0, \tilde{J}_q) e^{-kt/\tau_r(\tilde{J}_q)}, \end{aligned} \quad (10)$$

where the second line was obtained with the saddle point approximation (for derivation and prefactors γ_k see [98]). The time evolution of \mathcal{D}_t for various quenches is shown in Fig. 3a. Clearly, $\mathcal{D}_t \rightarrow 0$, implying that $\lim_{t \rightarrow \infty} V(m, \tilde{J}_q, t) = V_{\text{eq}}(m, \tilde{J}_q)$ almost everywhere, i.e. the large deviation behavior is ergodic [101, 102].

Dynamical phase diagram.—Due to asymptotic measure equivalence the dynamical phase transition may not always be easily observable, in particular if $t_c > \tau_r$. In Fig. 3b we present a dynamical phase diagram in the $(\tilde{J}_0, \tilde{J}_q)$ -plane, showing that the critical time

is not always smaller than the relaxation time. However, (i) there is an extended regime where $t_c < \tau_r$ (see blue region in Fig. 3b) such that the transition should be observable and (ii) the (exact) minimal relaxation time is always smaller than the (exact) smallest critical time and the latter always lies below the Néel point. The MF phase diagram is, however, starkly different (see [98]).

Conclusion.—Our results reveal, for the first time, the finite-time dynamical phase transition in nearest-neighbor interacting Ising systems. Moreover, they unravel non-trivial antiferromagnetic speed limits for the critical time and the relaxation time of the magnetization. Considering instead quenches from antiferromagnetically ordered states we in turn find mirror-symmetric results for the staggered magnetization [94–97]. These unforeseen speed limits embody an optimal trade-off between antiferromagnetic interactions biasing the magnetization towards smaller values, and a decreasing number of energetically accessible local configurations that impose kinetic constraints. As it emerges due to kinetic constraints imposed by frustrated local configurations, it

should not come as a surprise that the speed limit requires accounting for nearest-neighbor correlations and is therefore not captured by MF theory. Notably, speed limits may also be obtained from “classical” [66–72] or thermodynamic [68, 70, 73–75] speed limits which, however, is likely to be more difficult as analytical solutions for probability density functions, in particular at the critical time, do not seem to be feasible. Our findings may provide insight allowing for optimization of ultrafast optical-switching ferromagnetic materials [91]. Finally, our work provokes further intriguing questions, in particular on the microscopic path-wise understanding of the dynamical critical time, the effect of an external field, the existence of heating-cooling asymmetries [19–22] in different regimes and across phase transitions, and optimal driving protocols [15–18] that may be relevant for optical-switching ferromagnets.

Acknowledgments.—The financial support from the German Research Foundation (DFG) through the Emmy Noether Program GO 2762/1-2 (to AG) is gratefully acknowledged.

-
- [1] S. Dattagupta, *Relaxation phenomena in condensed matter physics* (Elsevier, 2012).
- [2] S. W. Wolfgang Haase, *Relaxation Phenomena* (Springer Berlin Heidelberg, 2003).
- [3] L. Onsager, *Phys. Rev.* **37**, 405 (1931).
- [4] L. Onsager, *Phys. Rev.* **38**, 2265 (1931).
- [5] R. Kubo, M. Yokota, and S. Nakajima, *J. Phys. Soc. Jpn.* **12**, 1203–1211 (1957).
- [6] U. Seifert and T. Speck, *EPL (Europhys. Lett.)* **89**, 10007 (2010).
- [7] M. Baiesi and C. Maes, *New J. Phys.* **15**, 013004 (2013).
- [8] W. Wu and J. Wang, *Front. Phys.* **8** (2020).
- [9] L. F. Cugliandolo, D. S. Dean, and J. Kurchan, *Phys. Rev. Lett.* **79**, 2168 (1997).
- [10] E. Lippiello, M. Baiesi, and A. Sarracino, *Phys. Rev. Lett.* **112**, 140602 (2014).
- [11] C. Maes, *Phys. Rep.* **850**, 1 (2020), frenesy: time-symmetric dynamical activity in nonequilibria.
- [12] Z. Lu and O. Raz, *Proc. Natl. Acad. Sci.* **114**, 5083 (2017).
- [13] I. Klich, O. Raz, O. Hirschberg, and M. Vucelja, *Phys. Rev. X* **9**, 021060 (2019).
- [14] A. Lasanta, F. Vega Reyes, A. Prados, and A. Santos, *Phys. Rev. Lett.* **119**, 148001 (2017).
- [15] D. M. Busiello, D. Gupta, and A. Maritan, *New Journal of Physics* **23**, 103012 (2021).
- [16] A. Gal and O. Raz, *Phys. Rev. Lett.* **124**, 060602 (2020).
- [17] P. R. Zulkowski and M. R. DeWeese, *Phys. Rev. E* **92**, 032117 (2015).
- [18] A. G. Frim, A. Zhong, S.-F. Chen, D. Mandal, and M. R. DeWeese, *Phys. Rev. E* **103**, L030102 (2021).
- [19] A. Lapolla and A. Godec, *Phys. Rev. Lett.* **125**, 110602 (2020).
- [20] J. Meibohm, D. Forastiere, T. Adeleke-Larodo, and K. Proesmans, *Phys. Rev. E* **104**, L032105 (2021).
- [21] S. K. Manikandan, *Phys. Rev. Research* **3**, 043108 (2021).
- [22] T. Van Vu and Y. Hasegawa, *Phys. Rev. Research* **3**, 043160 (2021).
- [23] R. Graham and T. Tél, *J. Stat. Phys.* **35**, 729–748 (1984).
- [24] R. Graham and T. Tél, *Phys. Rev. A* **31**, 1109 (1985).
- [25] F. Bouchet, K. Gawędzki, and C. Nardini, *J. Stat. Phys.* **163**, 1157–1210 (2016).
- [26] L. Bertini, A. De Sole, D. Gabrielli, G. Jona-Lasinio, and C. Landim, *Phys. Rev. Lett.* **87**, 040601 (2001).
- [27] L. Bertini, A. D. Sole, D. Gabrielli, G. Jona-Lasinio, and C. Landim, *J. Stat. Mech.* **2010**, L11001 (2010).
- [28] G. Bunin, Y. Kafri, and D. Podolsky, *J. Stat. Mech.* **2012**, L10001 (2012).
- [29] G. Bunin, Y. Kafri, and D. Podolsky, *J. Stat. Phys.* **152**, 112–135 (2013).
- [30] Y. Baek and Y. Kafri, *J. Stat. Mech.* **2015**, P08026 (2015).
- [31] J. P. Garrahan, R. L. Jack, V. Lecomte, E. Pitard, K. van Duijvendijk, and F. van Wijland, *Phys. Rev. Lett.* **98**, 195702 (2007).
- [32] J. P. Garrahan, R. L. Jack, V. Lecomte, E. Pitard, K. van Duijvendijk, and F. van Wijland, *J. Phys. A: Math. Theor.* **42**, 075007 (2009).
- [33] D. Chandler and J. P. Garrahan, *Annu. Rev. Phys. Chem.* **61**, 191 (2010).
- [34] J. P. Garrahan and I. Lesanovsky, *Phys. Rev. Lett.* **104**, 160601 (2010).
- [35] C. Ates, B. Olmos, J. P. Garrahan, and I. Lesanovsky, *Phys. Rev. A* **85**, 043620 (2012).
- [36] J. M. Hickey, C. Flindt, and J. P. Garrahan, *Phys. Rev. E* **90**, 062128 (2014).
- [37] R. L. Jack and P. Sollich, *J. Phys. A: Math. Theor.* **47**, 015003 (2013).
- [38] M. Gorissen, A. Lazarescu, K. Mallick, and C. Vanderzande, *Phys. Rev. Lett.* **109**, 170601 (2012).
- [39] C. P. Espigares, P. L. Garrido, and P. I. Hurtado, *Phys. Rev. E* **87**, 032115 (2013).
- [40] P. Tsobgni Nyawo and H. Touchette, *Phys. Rev. E* **94**, 032101 (2016).

- [41] N. Tizón-Escamilla, C. Pérez-Espigares, P. L. Garrido, and P. I. Hurtado, *Phys. Rev. Lett.* **119**, 090602 (2017).
- [42] J. Mehl, T. Speck, and U. Seifert, *Phys. Rev. E* **78**, 011123 (2008).
- [43] T. Speck, A. Engel, and U. Seifert, *J. Stat. Mech.* **2012**, P12001 (2012).
- [44] P. Tsobgni Nyawo and H. Touchette, *EPL (Europhysics Letters)* **116**, 50009 (2016).
- [45] R. L. Jack, I. R. Thompson, and P. Sollich, *Phys. Rev. Lett.* **114**, 060601 (2015).
- [46] R. J. Harris and H. Touchette, *J. Phys. A: Math. Theor.* **50**, 10LT01 (2017).
- [47] F. Barratt, A. B. Comas, P. Crowley, V. Oganessian, P. Sollich, and A. G. Green, *Phys. Rev. A* **103**, 052427 (2021).
- [48] P. Pietzonka, F. Ritort, and U. Seifert, *Phys. Rev. E* **96**, 012101 (2017).
- [49] A. Dechant, *J. Phys. A: Math. Theor.* **52**, 035001 (2018).
- [50] K. Liu, Z. Gong, and M. Ueda, *Phys. Rev. Lett.* **125**, 140602 (2020).
- [51] T. Koyuk and U. Seifert, *Phys. Rev. Lett.* **122**, 230601 (2019).
- [52] T. Koyuk and U. Seifert, *Phys. Rev. Lett.* **125**, 260604 (2020).
- [53] C. Dieball and A. Godec, *Direct route to thermodynamic uncertainty relations* (2022), arXiv:2208.06402 [cond-mat.stat-mech].
- [54] L. Mandelstam and I. Tamm, *J. Phys. USSR* **9** (1945).
- [55] K. Bhattacharyya, *J. Phys. A: Math. Gen.* **16**, 2993–2996 (1983).
- [56] J. Anandan and Y. Aharonov, *Phys. Rev. Lett.* **65**, 1697 (1990).
- [57] P. Pfeifer, *Phys. Rev. Lett.* **70**, 3365 (1993).
- [58] N. Margolus and L. B. Levitin, *Physica D* **120**, 188 (1998).
- [59] S. Lloyd, *Nature* **406**, 1047–1054 (2000).
- [60] V. Giovannetti, S. Lloyd, and L. Maccone, *Phys. Rev. A* **67**, 052109 (2003).
- [61] S. Deffner and E. Lutz, *J. Phys. A: Math. Theor.* **46**, 335302 (2013).
- [62] M. M. Taddei, B. M. Escher, L. Davidovich, and R. L. de Matos Filho, *Phys. Rev. Lett.* **110**, 050402 (2013).
- [63] A. del Campo, I. L. Egusquiza, M. B. Plenio, and S. F. Huelga, *Phys. Rev. Lett.* **110**, 050403 (2013).
- [64] S. Deffner and E. Lutz, *Phys. Rev. Lett.* **111**, 010402 (2013).
- [65] L. P. García-Pintos, S. B. Nicholson, J. R. Green, A. del Campo, and A. V. Gorshkov, *Phys. Rev. X* **12**, 011038 (2022).
- [66] M. Okuyama and M. Ohzeki, *Phys. Rev. Lett.* **120**, 070402 (2018).
- [67] B. Shanahan, A. Chenu, N. Margolus, and A. del Campo, *Phys. Rev. Lett.* **120**, 070401 (2018).
- [68] N. Shiraishi, K. Funo, and K. Saito, *Phys. Rev. Lett.* **121**, 070601 (2018).
- [69] E. Aurell, C. Mejía-Monasterio, and P. Muratore-Ginanneschi, *Phys. Rev. Lett.* **106**, 250601 (2011).
- [70] S. Ito and A. Dechant, *Phys. Rev. X* **10**, 021056 (2020).
- [71] E. Aurell, K. Gawędzki, C. Mejía-Monasterio, R. Mohayaei, and P. Muratore-Ginanneschi, *J. Stat. Phys.* **147**, 487–505 (2012).
- [72] V. T. Vo, T. Van Vu, and Y. Hasegawa, *Phys. Rev. E* **102**, 062132 (2020).
- [73] G. Falasco and M. Esposito, *Phys. Rev. Lett.* **125**, 120604 (2020).
- [74] N. Shiraishi and K. Saito, *Phys. Rev. Lett.* **123**, 110603 (2019).
- [75] K. Yoshimura and S. Ito, *Phys. Rev. Lett.* **127**, 160601 (2021).
- [76] J. Meibohm and M. Esposito, *Phys. Rev. Lett.* **128**, 110603 (2022).
- [77] J. Meibohm and M. Esposito, arXiv preprint arXiv:2205.10311 (2022).
- [78] C. Külske and A. Le Ny, *Commun. Math. Phys.* **271**, 431–454 (2007).
- [79] V. Ermolaev and C. Külske, *J. Stat. Phys.* **141**, 727–756 (2010).
- [80] In [77] only super-critical quench temperatures $T_q > T_c$ are considered, whereas [78, 79] consider all possible T_q .
- [81] A. Bray, *Physica A* **194**, 41 (1993).
- [82] H. A. Bethe, *Proc. Math. Phys. Eng. Sci.* **150**, 552 (1935).
- [83] E. A. Guggenheim, *Proc. Math. Phys. Eng. Sci.* **148**, 304 (1935).
- [84] K. Blom and A. Godec, *Phys. Rev. X* **11**, 031067 (2021).
- [85] In [76, 78, 79] there is no explicit dependence on the lattice coordination number \bar{z} . This is equivalent to setting $\bar{z} = 1$ in this work.
- [86] K. Kawasaki, *Phys. Rev.* **145**, 224 (1966).
- [87] L. P. Kadanoff and J. Swift, *Phys. Rev.* **165**, 310 (1968).
- [88] Y. Saito and R. Kubo, *J. Stat. Phys.* **15**, 233 (1976).
- [89] M. I. Dykman, E. Mori, J. Ross, and P. M. Hunt, *J. Chem. Phys.* **100**, 5735 (1994).
- [90] A. Imparato and L. Peliti, *Phys. Rev. E* **72**, 046114 (2005).
- [91] J. Chatterjee, D. Polley, A. Pattabi, H. Jang, S. Salahuddin, and J. Bokor, *Adv. Funct. Mater.* **32**, 2107490 (2022).
- [92] P. Hakonen and O. V. Lounasmaa, *Science* **265**, 1821 (1994).
- [93] Note that only the nuclear spin temperature becomes negative, other degrees of freedom actually heat up. For an excellent pedagogical expose on negative temperatures in systems with bounded energy spectra see [109].
- [94] J. M. Ziman, *Proc. Phys. Soc. A* **64**, 1108 (1951).
- [95] S. Katsura and M. Takizawa, *Prog. Theor. Exp. Phys.* **51**, 82 (1974).
- [96] I. Ono, *J. Phys. C Solid State Phys.* **17**, 3615 (1984).
- [97] F. Peruggi, F. di Liberto, and G. Monroy, *J. Phys. A Math. Theor.* **16**, 811 (1983).
- [98] See Supplemental Material at [...] for detailed derivations and auxiliary results.
- [99] E. R. Love, *Math. Gaz.* **64**, 55 (1980).
- [100] The mean magnetization $\lim_{N \rightarrow \infty} \langle m_t \rangle$ is evaluated with the saddle-point method yielding contributions from the free energy minima. In the two-phase regime $\tilde{f}(m, \vec{J})$ has two global minima equidistant from $m = 0$. Therefore $\lim_{N \rightarrow \infty} \langle m_t \rangle = 0$.
- [101] T. Squartini, J. de Mol, F. den Hollander, and D. Garlaschelli, *Phys. Rev. Lett.* **115**, 268701 (2015).
- [102] H. Touchette, *J. Stat. Phys.* **159**, 987 (2015).
- [103] J. L. Lebowitz and P. G. Bergmann, *Ann. Phys. (N. Y.)* **1**, 1 (1957).
- [104] M. C. Mackey, *Rev. Mod. Phys.* **61**, 981 (1989).
- [105] H. Qian, *J. Math. Phys.* **54**, 053302 (2013).
- [106] C. Van den Broeck and M. Esposito, *Phys. Rev. E* **82**, 011144 (2010).
- [107] M. Esposito and C. Van den Broeck, *Phys. Rev. Lett.* **104**, 090601 (2010).

- [108] S. Vaikuntanathan and C. Jarzynski, *EPL* **87**, 60005 (2009).
- [109] D. Frenkel and P. B. Warren, *Am. J. Phys.* **83**, 163–170 (2015).

**Supplemental Material for:
Global Speed Limit for Finite-Time Dynamical Phase Transition in Nonequilibrium Relaxation**

Kristian Blom & Aljaž Godec

Mathematical bioPhysics group, Max Planck Institute for Multidisciplinary Sciences, Göttingen 37077, Germany

In this Supplementary Material (SM) we present details of the calculations, auxiliary results, and mathematical proofs of the claims made in the Letter. The sections are organized in the order they appear in the Letter.

CONTENTS

S1. Hamiltonian formalism	1
S2. Lagrangian formalism	2
S3. Derivation of the critical time	2
A. Hamiltonian formalism and the Ricatti equation	2
B. Lagrangian formalism and the symmetry-breaking transition	3
S4. Bounds on the BG critical time	4
A. $\tilde{J}_q < \tilde{J}_c^{\text{BG}}$	4
B. $\tilde{J}_q \geq \tilde{J}_c^{\text{BG}}$	5
1. $\mathcal{A}_2(\tilde{J}_q, \tilde{J}_0) > 1 \forall \tilde{J}_q > \tilde{J}_c^{\text{BG}}$	5
2. $\mathcal{A}_1(\tilde{J}_0, \tilde{J}_q) > 0 \forall \tilde{J}_q > \tilde{J}_c^{\text{BG}}$	6
S5. Relaxation dynamics	6
A. BG approximation with $\bar{z} = 2$	6
B. BG approximation with $\bar{z} = 4$	7
1. $\tilde{J}_q < \ln(2)/2$ and $\tilde{J}_q \neq \ln(2)/4$	7
2. $\tilde{J}_q = \ln(2)/4$	8
3. $\tilde{J}_q > \ln(2)/2$	9
S6. Relative entropy	10
S7. Parity symmetry for the staggered magnetization	10
S8. MF dynamical phase diagram	11
References	11

S1. HAMILTONIAN FORMALISM

Recall that $V(m, \tilde{J}, t) \equiv -\lim_{N \rightarrow \infty} N^{-1} \ln(P_N(m, \tilde{J}, t))$ represents the time-dependent large-deviation rate function. In the SM of [1] it is shown that the rate function $V(m, \tilde{J}_q, t)$ with quench temperature/coupling \tilde{J}_q obeys the Hamilton-Jacobi (HJ) equation given by Eq. (5) in the main Letter. The HJ equation can be solved with the *method of characteristics* as follows: Let $\{q(s), p(s)\}$ $0 \leq s \leq t$ be the characteristics that solve the Hamilton's equations

$$\dot{q}(s) = \partial_p \mathcal{H}(q, p), \quad \dot{p}(s) = -\partial_q \mathcal{H}(q, p), \quad q(t) = m, \quad p(0) = \tilde{f}'(q(0), \tilde{J}_0), \quad (\text{S1})$$

where $\dot{q}(s) \equiv dq(s)/ds$, $\dot{p}(s) \equiv dp(s)/ds$, $\tilde{f}'(a, \tilde{J}) \equiv \partial_m \tilde{f}(m, \tilde{J})|_{m=a}$, and $\mathcal{H}(q, p)$ is given in Eq. (6) in the Letter. Upon solving the Hamilton's equations, the solution to the HJ equation reads

$$V(m, \tilde{J}_q, t) = \int_0^t [p(s)\dot{q}(s) - \mathcal{H}(q, p)]ds + V(q(0), \tilde{J}_0, 0). \quad (\text{S2})$$

For $t > t_c$, where $t_c = t_c(\tilde{J}_0, \tilde{J}_q)$ denotes the critical time, the solutions to the Hamilton's equations become degenerate. Under these circumstances, the solution that minimizes Eq. (S2) corresponds to the stable solution [2].

S2. LAGRANGIAN FORMALISM

One can also obtain the solution to the HJ equation with the Lagrangian formalism, which is formally introduced in [3, 4]. The Lagrangian is obtained from the Hamiltonian via the backward Legendre transform $\mathcal{L}(q, \dot{q}) = p(q, \dot{q})\dot{q} - \mathcal{H}(q, p(q, \dot{q}))$, where $p(q, \dot{q})$ can be obtained from the first of the Hamilton's equations in Eq. (S1) and reads

$$p(q, \dot{q}) = \frac{1}{2} \ln \left(\frac{\dot{q} + \Lambda(q, \dot{q})}{4w^+(q, \tilde{J}_q)} \right), \quad (\text{S3})$$

with $\Lambda(q, \dot{q}) \equiv [16w^+(q, \tilde{J}_q)w^-(q, \tilde{J}_q) + \dot{q}^2]^{1/2}$. Plugging this expression back into $\mathcal{H}(q, p(q, \dot{q}))$ we obtain the Lagrangian

$$\mathcal{L}(q, \dot{q}) = p(q, \dot{q})\dot{q} - \Lambda(q, \dot{q})/2 + w^+(q, \tilde{J}_q) + w^-(q, \tilde{J}_q). \quad (\text{S4})$$

The Hamilton's equations are replaced by the Euler-Lagrange (EL) equation, which reads

$$\ddot{q}(s) = 2\Lambda(q, \dot{q})\partial_q[w^+(q, \tilde{J}_q) + w^-(q, \tilde{J}_q)] - 8\partial_q w^+(q, \tilde{J}_q)w^-(q, \tilde{J}_q), \quad \dot{q}(0) = g(q(0)), \quad q(t) = m. \quad (\text{S5})$$

The boundary condition for $\dot{q}(0)$ is determined by the *curve of allowed initial configurations* (see also Eq. (24) in [4])

$$g(m) \equiv 2 \exp(2\tilde{f}'(m, \tilde{J}_0))w^+(m, \tilde{J}_q) - 2 \exp(-2\tilde{f}'(m, \tilde{J}_0))w^-(m, \tilde{J}_q), \quad (\text{S6})$$

which will be used in Sec. S3B to determine the symmetry-breaking transition. Upon solving the EL equation, the solution of the HJ equation is given by

$$V(m, \tilde{J}_q, t) = \int_0^t \mathcal{L}(q(s), \dot{q}(s))ds + V(q(0), \tilde{J}_0, 0), \quad (\text{S7})$$

which is identical to Eq. (S2). Similar to the Hamiltonian formalism, the solution of Eq. (S5) becomes degenerate for $t > t_c$. The stable solution for $q(s)$ minimizes the rate function given by Eq. (S7).

S3. DERIVATION OF THE CRITICAL TIME

In this section we derive the critical time t_c based on two different approaches which are discussed in [1] and [4], respectively. The first approach uses the Hamiltonian formalism discussed in Sec. S1 to derive an equation for the curvature at $m = 0$. The second approach uses an invariance principle for the solutions of Eq. (S5) discussed in Sec. S2. Both approaches lead to the same result for the critical time given by Eq. (7) in the main Letter. However, with the latter approach we can also derive the initial temperature below which the initial location of the cusp deviates from $m = 0$.

A. Hamiltonian formalism and the Riccati equation

The critical time $t_c(\tilde{J}_0, \tilde{J}_q)$ is defined as the moment when the rate function $V(m, \tilde{J}_q, t)$ develops a cusp at $m = 0$, leading to a negatively diverging curvature. In the SM of [1] an equation for the curvature $V_0''(\tilde{J}_q, t) \equiv V''(0, \tilde{J}_q, t)$ is derived from the Hamilton's equations. The resulting equation – after simplification – reads

$$\frac{dV_0''(\tilde{J}_q, t)}{dt} = 8w^\pm(0, \tilde{J}_q)V_0''(\tilde{J}_q, t)(\tilde{f}''(0, \tilde{J}_q) - V_0''(\tilde{J}_q, t)), \quad (\text{S8})$$

with initial condition $V_0''(\tilde{J}_q, 0) = \tilde{f}''(0, \tilde{J}_0)$. To obtain Eq. (S8) we explicitly used the detailed-balance relation $\ln(w^-(m, \tilde{J})/w^+(m, \tilde{J})) = 2\tilde{f}'(m, \tilde{J})$ and the parity symmetry $w^\pm(m, \tilde{J}) = w^\mp(-m, \tilde{J})$ to write $\partial_m w^\pm(m, \tilde{J})|_{m=0} = \mp w^\pm(0, \tilde{J})\tilde{f}''(0, \tilde{J})$. Eq. (S8) is a so-called *Riccati equation*, which can be solved analytically. The resulting solution up to the critical time reads

$$V_0''(\tilde{J}_q, t) = \frac{\tilde{f}''(0, \tilde{J}_q)}{1 - (1 - \tilde{f}''(0, \tilde{J}_q)/\tilde{f}''(0, \tilde{J}_0))e^{-2t/\hat{\tau}_r(\tilde{J}_q)}}, \quad (\text{S9})$$

where $1/\hat{\tau}_r(\tilde{J}_q) \equiv 4w^\pm(0, \tilde{J}_q)\tilde{f}''(0, \tilde{J}_q)$ is an effective relaxation rate. The critical time t_c determines the root of the denominator in Eq. (S9). Solving for the root leads to Eq. (7) in the main Letter.

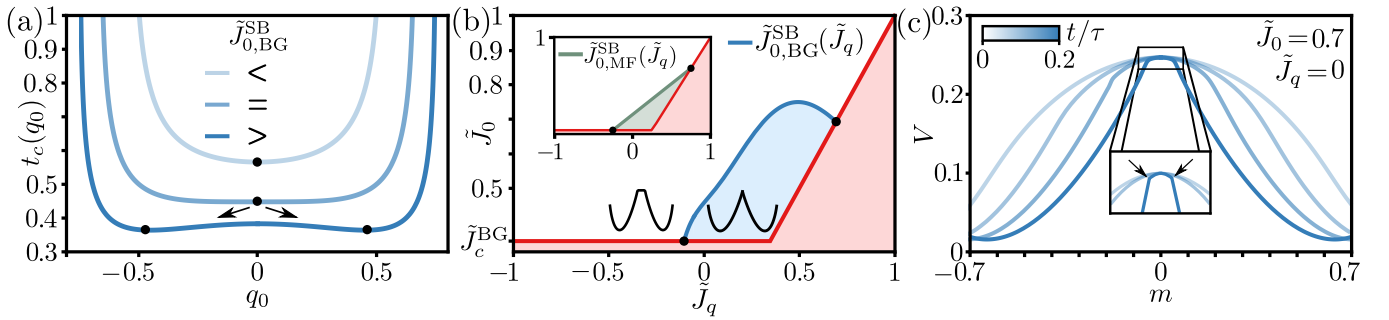


FIG. S1. **Symmetry-breaking transition for the location of the cusp.** In all panels we consider a lattice with $\bar{z} = 4$. (a) BG critical time $t_c^{\text{BG}}(q_0)$ given by Eq. (S13) as a function of the initial point q_0 for various values of the initial temperature \tilde{J}_0 . The black dots indicate the minima of $t_c^{\text{BG}}(q_0)$, which set the location of the cusp. For $\tilde{J}_0 > \tilde{J}_{0,\text{BG}}^{\text{SB}}$ the critical time contains two minima $\pm q_{\text{min}}$ (black dots), which correspond to non-zero cusp locations. (b) Blue line: BG symmetry-breaking temperature $\tilde{J}_0^{\text{SB}}(\tilde{J}_q)$ given by Eq. (S16) as a function of the quench temperature \tilde{J}_q . Inside the light blue region the cusp is formed at $m = 0$, and in the white region the cusp is formed at $m \neq 0$. The red area is forbidden since $\tilde{J}_0 > \tilde{J}_c^{\text{BG}}$ and $\tilde{J}_q < \tilde{J}_0$. Inset: MF symmetry-breaking temperature $\tilde{J}_0^{\text{MF}}(\tilde{J}_q)$ given by Eq. (S15). Inside the light green region the cusp is formed at $m = 0$. (c) Temporal evolution of the BG rate function $V_{\text{BG}}(m, \tilde{J}_q, t)$ for a quench to $\tilde{J}_q = 0$. Time increases from light to dark blue. The initial temperature is set below the the symmetry-breaking temperature, i.e. $\tilde{J}_0 > \tilde{J}_0^{\text{SB}}(\tilde{J}_q)$, to induce a cusp at $m \neq 0$. Inset: Enlargement of the rate function around the center. Black arrows indicate the location of the cusps.

B. Lagrangian formalism and the symmetry-breaking transition

Following the steps in Sec. 3.5 of [4] we can derive the critical temperature $\tilde{J}_0^{\text{SB}}(\tilde{J}_q)$, below which the initial location of the cusp deviates from $\bar{m} = 0$. The idea behind this calculation is that at the critical time the solution of Eq. (S5) converges to the same point $q(t_c)$ for *different initial conditions* $\{q(0), \dot{q}(0)\}$. In other words, *the location of $q(t_c)$ remains invariant under a variation of the initial conditions*. To determine the symmetry-breaking transition it suffices to consider the dynamics of $q(s)$ around the origin [4]. We linearize Eq. (S5) around the point $(q, \dot{q}) = (0, 0)$, which yields

$$\ddot{q}(s) = q(s)/\hat{\tau}_r^2(\tilde{J}_q), \quad \dot{q}(0) = g(q_0) \equiv v_0, \quad q(0) \equiv q_0, \quad (\text{S10})$$

where $\{q_0, v_0(q_0)\}$ are the initial conditions, and $1/\hat{\tau}_r(\tilde{J}_q) \equiv 4w^\pm(0, \tilde{J}_q)\tilde{f}''(0, \tilde{J}_q)$. The solution of Eq. (S10) is given by

$$q(s) = (q_0/2 - \hat{\tau}_r v_0/2)e^{-s/\hat{\tau}_r} + (q_0/2 + \hat{\tau}_r v_0/2)e^{s/\hat{\tau}_r}. \quad (\text{S11})$$

We now consider a variation of $q(s)$ w.r.t. the initial conditions $\{q_0, v_0(q_0)\}$, which gives

$$\frac{dq(s)}{dq_0} = \frac{\partial q(s)}{\partial q_0} + \frac{\partial q(s)}{\partial v_0} g'(q_0) = (1/2 - \hat{\tau}_r g'(q_0)/2)e^{-s/2\hat{\tau}_r} + (1/2 + \hat{\tau}_r g'(q_0)/2)e^{s/2\hat{\tau}_r}, \quad (\text{S12})$$

where $g'(q_0) \equiv dg(m)/dm|_{m=q_0}$ and $g(m)$ is given by Eq. (S6). At the critical time $s = t_c$ the variation (S12) vanishes, which leads to the the critical time in the form

$$t_c(q_0) = (\hat{\tau}_r/2) \ln \left(\frac{g'(q_0) - 1/\hat{\tau}_r}{g'(q_0) + 1/\hat{\tau}_r} \right). \quad (\text{S13})$$

For $\tilde{J}_c < \tilde{J}_0 < \tilde{J}_0^{\text{SB}}(\tilde{J}_q)$ the critical time given by Eq. (S13) has a single minimum at $q_{\text{min}} = 0$ (see upper line in Fig. S1a). Inserting $q_0 = 0$ and recalling the relation $\partial_m w^\pm(m, \tilde{J})|_{m=0} = \mp w^\pm(0, \tilde{J})\tilde{f}''(0, \tilde{J})$ we obtain the critical time given by Eq. (7) in the main Letter.

For $\tilde{J}_0 > \tilde{J}_0^{\text{SB}}(\tilde{J}_q)$ Eq. (S13) develops two minima at $\pm q_{\text{min}} \neq 0$, *corresponding to the new cusp locations* (see lower line in Fig. S1a).

For $\tilde{J}_0 = \tilde{J}_0^{\text{SB}}(\tilde{J}_q)$ the curvature of Eq. (S13) at $q_0 = 0$ vanishes (see middle line in Fig. S1a), which results in the following equation determining $\tilde{J}_0^{\text{SB}}(\tilde{J}_q)$

$$g'''(0)|_{\tilde{J}_0^{\text{SB}}(\tilde{J}_q)} = 0, \quad (\text{S14})$$

where we have used that $g''(0) = 0$. Solving Eq. (S14) for the MF approximation we obtain the simple result

$$\tilde{J}_{0,\text{MF}}^{\text{SB}}(\tilde{J}_q) = \frac{3 + \bar{z}\tilde{J}_q}{2\bar{z}}. \quad (\text{S15})$$

For $\tilde{J}_q = 0$ we obtain $\tilde{J}_{0,\text{MF}}^{\text{SB}}(0) = 3/2z$ as mentioned in [3, 4]. Note that there is a typo in Eq. (41) in [4]. For the BG approximation the general formula for $\tilde{J}_{0,\text{BG}}^{\text{SB}}(\tilde{J}_q)$ is rather long and therefore not shown. For $\bar{z} = 4$ the result can compactly be written as

$$\tilde{J}_{0,\text{BG}}^{\text{SB}}(\tilde{J}_q)|_{z=4} = \ln(x_{\tilde{J}_q})/2, \quad (\text{S16})$$

where $x_{\tilde{J}_q}$ is the *real solution* of the following cubic equation

$$20 - 16(1 + 2e^{-2\tilde{J}_q})x_{\tilde{J}_q} + (8 + 8e^{-2\tilde{J}_q} + 20e^{-4\tilde{J}_q})x_{\tilde{J}_q}^2 - (2 - 4e^{-2\tilde{J}_q} + 10e^{-4\tilde{J}_q} - e^{-8\tilde{J}_q} + 6e^{-10\tilde{J}_q} - 9e^{-12\tilde{J}_q} + 4e^{-14\tilde{J}_q})x_{\tilde{J}_q}^3 = 0. \quad (\text{S17})$$

For $\tilde{J}_q = 0$ we obtain $\tilde{J}_{0,\text{BG}}^{\text{SB}}(0) = \ln(\frac{\bar{z}+1}{\bar{z}-2})/2$ as mentioned in the main Letter. In Fig. S1b we plot Eq. (S16) as a function of \tilde{J}_0 with the dark blue line. Interestingly, the light blue region for which the cusp appears at $m = 0$ is rather small and of finite area. Correspondingly, in Fig. S1c we provide an example of the rate function $V_{\text{BG}}(m, \tilde{J}_q, t)$ for which the cusps appear at a non-zero locations.

S4. BOUNDS ON THE BG CRITICAL TIME

In this section we derive the bounds for the BG critical time t_c^{BG} . Inserting the BG free energy density and transition rates – given by Eqs. (2) and (4) in the main Letter – into Eq. (7) in the main Letter, we obtain

$$t_c^{\text{BG}}(\tilde{J}_0, \tilde{J}_q) = \frac{\cosh^{\bar{z}}(\tilde{J}_q)(\tanh(\tilde{J}_q) + 1)}{4((\bar{z} - 1)\tanh(\tilde{J}_q) - 1)} \left[\tilde{J}_q + \ln \left(\frac{(\bar{z} - 1)\sinh(\tilde{J}_0) - \cosh(\tilde{J}_0)}{\bar{z}\sinh(\tilde{J}_0 - \tilde{J}_q)} \right) \right], \quad (\text{S18})$$

where $\tilde{J}_0 > \tilde{J}_c^{\text{BG}} \equiv \ln(\bar{z}/(\bar{z} - 2))/2$ and $\tilde{J}_q \leq \tilde{J}_0$. Fig. 2(c) in the main Letter displays the BG critical given by Eq. (S18) with the blue line. The BG critical time has a minimum for an anti-ferromagnetic quench $\tilde{J}_q < 0$, which cannot be determined analytically. We can, however, derive lower bounds on the critical time. To construct the bounds we will distinguish between quenches in the one- and two-phase domain, i.e. $\tilde{J}_q < \tilde{J}_c^{\text{BG}}$ and $\tilde{J}_q \geq \tilde{J}_c^{\text{BG}}$. The general result for the anti-ferromagnetic bound is given by Eq. (8) in the Letter.

A. $\tilde{J}_q < \tilde{J}_c^{\text{BG}}$

For quenches in the one-phase domain we can bound the critical time by applying the well-known inequality $\ln(1 + x) > 2x/(2 + x)$ for $x > 0$ [5] to the logarithmic term in Eq. (7) in the main Letter (since $-\tilde{f}_{\text{BG}}''(0, \tilde{J}_q)/\tilde{f}_{\text{BG}}''(0, \tilde{J}_0) > 0$). This yields the *local* lower bound

$$t_c^{\dagger\text{BG}}(\tilde{J}_0, \tilde{J}_q) = \frac{\cosh^{\bar{z}}(\tilde{J}_q)}{\bar{z} - 2 + \bar{z}e^{-2\tilde{J}_q} - 2\bar{z}e^{-2\tilde{J}_0}}. \quad (\text{S19})$$

In Fig. S2a we plot $t_c^{\dagger\text{BG}}$ with the black line. Surprisingly, this local bound also seems to work for $\tilde{J}_q \geq \tilde{J}_c^{\text{BG}}$, even though $-\tilde{f}_{\text{BG}}''(0, \tilde{J}_q)/\tilde{f}_{\text{BG}}''(0, \tilde{J}_0) < 0$. Furthermore, it gives the exact result for $\tilde{J}_q = \tilde{J}_c^{\text{BG}}$ given by Eq. (S21). The lower bound is also non-monotonic w.r.t. \tilde{J}_q , and displays a minimum for an anti-ferromagnetic quench $\tilde{J}_q < 0$. At the respective minimum, the *global* lower bound $\inf_{\tilde{J}_q} t_c^{\dagger\text{BG}}(\tilde{J}_0, \tilde{J}_q)$ (see black dashed line in Fig. S2a) is given by Eq. (8) in the main Letter.

Taking the limit $\tilde{J}_0 \rightarrow \infty$ of Eq. (8), we further obtain the following universal global lower bound independent of \tilde{J}_q and \tilde{J}_0 that reads

$$\lim_{\tilde{J}_0 \rightarrow \infty} \inf_{\tilde{J}_q} t_c^{\dagger\text{BG}}(\tilde{J}_0, \tilde{J}_q) = \frac{(\bar{z} - 2)^{1-\bar{z}/2} [2 + \nu_{\bar{z}}]^{-\bar{z}/2} [\bar{z} + \nu_{\bar{z}}]^{\bar{z}}}{2^{\bar{z}} (4 + \bar{z}[\bar{z} - 2 + \nu_{\bar{z}}])}, \quad (\text{S20})$$

with $\nu_{\bar{z}} \equiv \sqrt{8 + \bar{z}(\bar{z} - 4)}$. For $\bar{z} = 4$ this gives the universal global lower bound $t_c^{\dagger\text{BG}}(\tilde{J}_0, \tilde{J}_q) > 1/8$ and is shown with the red line in Fig. S2a. In Fig. S2b we observe that for increasing \bar{z} the bounds given by Eq. (8) in the main Letter and Eq. (S20) become sharper with respect to the true/exact minimum of t_c^{BG} .

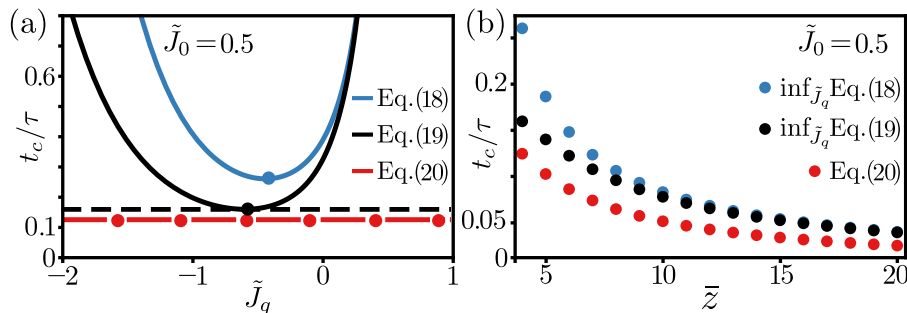


FIG. S2. **Bounds on the BG critical time for quenches in the one-phase domain.** (a) BG critical time $t_c^{\text{BG}}(\tilde{J}_0, \tilde{J}_q)$ given by Eq. (S18) (blue line) as a function of the quench temperature \tilde{J}_q for $\tilde{J}_0 = 0.5$ and $\bar{z} = 4$. The respective lower bounds are shown with the black and red line. (b) Minimum of the BG critical time (blue dots) as a function of the lattice coordination number \bar{z} . The respective lower bounds are shown with the black and red dots, respectively.

B. $\tilde{J}_q \geq \tilde{J}_c^{\text{BG}}$

For quenches in the two-phase domain we prove that the BG critical time $t_c^{\text{BG}}(\tilde{J}_0, \tilde{J}_q)$ is bounded from below by the critical quench $t_c^{\text{BG}}(\tilde{J}_0, \tilde{J}_c^{\text{BG}})$, which reads

$$t_c^{\text{BG}}(\tilde{J}_0, \tilde{J}_c^{\text{BG}}) = \left(\frac{\bar{z} - 1}{\sqrt{\bar{z}(\bar{z} - 2)}} \right)^{\bar{z}} \frac{\tanh(\tilde{J}_0) + 1}{4((\bar{z} - 1) \tanh(\tilde{J}_0) - 1)}. \quad (\text{S21})$$

To prove that Eq. (S21) provides a lower bound for the critical time for quenches in the two-phase domain, we first differentiate Eq. (S18) w.r.t. \tilde{J}_q , which gives

$$\frac{\partial t_c^{\text{BG}}(\tilde{J}_0, \tilde{J}_q)}{\partial \tilde{J}_q} = \frac{\bar{z}(1 + \tanh(\tilde{J}_q)) \cosh^{\bar{z}}(\tilde{J}_q)}{4((\bar{z} - 1) \tanh(\tilde{J}_q) - 1)^2} \mathcal{A}_1(\tilde{J}_0, \tilde{J}_q), \quad (\text{S22})$$

where we have introduced the auxiliary function (and subsequent auxiliary functions)

$$\begin{aligned} \mathcal{A}_1(\tilde{J}_0, \tilde{J}_q) &\equiv -\mathcal{A}_2(\tilde{J}_0, \tilde{J}_q)[1 - \tanh(\tilde{J}_q)] - \mathcal{A}_3(\tilde{J}_q) \ln(\mathcal{A}_2(\tilde{J}_q, \tilde{J}_0)), \\ \mathcal{A}_2(\tilde{J}_0, \tilde{J}_q) &\equiv [(\bar{z} - 1) \tanh(\tilde{J}_q) - 1][1 + \tanh(\tilde{J}_0)] / [\bar{z}(\tanh(\tilde{J}_q) - \tanh(\tilde{J}_0))], \\ \mathcal{A}_3(\tilde{J}_q) &\equiv 1 - (\bar{z} - 1) \tanh^2(\tilde{J}_q). \end{aligned} \quad (\text{S23})$$

All terms in front of $\mathcal{A}_1(\tilde{J}_0, \tilde{J}_q)$ in Eq. (S22) are trivially positive. If furthermore $\mathcal{A}_1(\tilde{J}_0, \tilde{J}_q) > 0$ for $\tilde{J}_c^{\text{BG}} < \tilde{J}_q < \tilde{J}_0$, then we know that Eq. (S21) provides a lower bound. To prove that the latter is positive we proceed in two steps.

1. $\mathcal{A}_2(\tilde{J}_q, \tilde{J}_0) > 1 \forall \tilde{J}_q > \tilde{J}_c^{\text{BG}}$

First we focus on the term $\mathcal{A}_2(\tilde{J}_q, \tilde{J}_0)$ entering the logarithm in $\mathcal{A}_1(\tilde{J}_0, \tilde{J}_q)$. Here we prove that $\mathcal{A}_2(\tilde{J}_q, \tilde{J}_0) > 1 \forall \tilde{J}_q > \tilde{J}_c^{\text{BG}}$, which we need for the second step. First, note that $\mathcal{A}_2(\tilde{J}_c^{\text{BG}}, \tilde{J}_0) = 1$, which can easily be checked by hand. Introducing $x_0 \equiv \tanh(\tilde{J}_0)$ and $x_q \equiv \tanh(\tilde{J}_q)$, we find $\partial_{\tilde{J}_q} \mathcal{A}_2(\tilde{J}_q, \tilde{J}_0) = \cosh^{-2}(\tilde{J}_q) \partial_{x_q} \mathcal{A}_2(x_q, x_0) > 0 \forall \tilde{J}_0 > \tilde{J}_c^{\text{BG}}$. To see this, we write out the partial derivative and obtain

$$\partial_{x_q} \mathcal{A}_2(x_q, x_0) = \partial_{x_q} \left(\frac{(1 + x_q)[(\bar{z} - 1)x_0 - 1]}{\bar{z}(x_0 - x_q)} \right) = \frac{(1 + x_0)((\bar{z} - 1)x_0 - 1)}{\bar{z}(x_0 - x_q)^2} > 0 \forall x_0 > (\bar{z} - 1)^{-1}. \quad (\text{S24})$$

Finally, note that $x_0 > (\bar{z} - 1)^{-1}$ translates to $\tilde{J}_0 > \text{arctanh}((\bar{z} - 1)^{-1}) = \tilde{J}_c^{\text{BG}}$, which is the regime of interest. Hence, $\mathcal{A}_2(\tilde{J}_q, \tilde{J}_0)$ has a positive slope w.r.t. \tilde{J}_q . Combined with $\mathcal{A}_2(\tilde{J}_c^{\text{BG}}, \tilde{J}_0) = 1$, this proves that $\mathcal{A}_2(\tilde{J}_q, \tilde{J}_0) > 1 \forall \tilde{J}_q > \tilde{J}_c^{\text{BG}}$.

$$2. \mathcal{A}_1(\tilde{J}_0, \tilde{J}_q) > 0 \quad \forall \tilde{J}_q > \tilde{J}_c^{\text{BG}}$$

Now we turn our attention to $\mathcal{A}_1(\tilde{J}_0, \tilde{J}_q)$. We begin by considering the regime $\tanh(\tilde{J}_q) \geq 1/\sqrt{z-1}$. Here $\mathcal{A}_3(\tilde{J}_q) < 0$, and therefore $-\mathcal{A}_3(\tilde{J}_q) \ln(\mathcal{A}_2(\tilde{J}_q, \tilde{J}_0)) > 0$ based on the previous step. Furthermore, $-\mathcal{A}_2(\tilde{J}_0, \tilde{J}_q)[1 - \tanh(\tilde{J}_q)] > 0 \quad \forall \tilde{J}_c^{\text{BG}} < \tilde{J}_q < \tilde{J}_0$, and so it follows that $\mathcal{A}_1(\tilde{J}_0, \tilde{J}_q) > 0$ for $1/\sqrt{z-1} \leq \tanh(\tilde{J}_q) \leq \tanh(\tilde{J}_0)$.

Next we consider the regime $1/(z-1) < \tanh(\tilde{J}_q) < 1/\sqrt{z-1}$. Here $\mathcal{A}_3(\tilde{J}_q) > 0$, and therefore $-\mathcal{A}_3(\tilde{J}_q) \ln(\mathcal{A}_2(\tilde{J}_q, \tilde{J}_0)) < 0$. To construct a bound for $\mathcal{A}_1(\tilde{J}_0, \tilde{J}_q)$ we apply the following chain of inequalities

$$\begin{aligned} \mathcal{A}_1(\tilde{J}_0, \tilde{J}_q) &\equiv \mathcal{A}_3(\tilde{J}_q)[- \mathcal{A}_2(\tilde{J}_0, \tilde{J}_q)[1 - \tanh(\tilde{J}_q)] / \mathcal{A}_3(\tilde{J}_q) - \ln(\mathcal{A}_2(\tilde{J}_q, \tilde{J}_0))] \\ &> \mathcal{A}_3(\tilde{J}_q)[- \mathcal{A}_2(\tilde{J}_0, \tilde{J}_q)[1 - \tanh(\tilde{J}_q)] / \mathcal{A}_3(\tilde{J}_q) - \mathcal{A}_2(\tilde{J}_q, \tilde{J}_0) + 1] \\ &> \mathcal{A}_3(\tilde{J}_q)[- \mathcal{A}_2(\tilde{J}_0, \tilde{J}_q) - \mathcal{A}_2(\tilde{J}_q, \tilde{J}_0) + 1] = 0. \end{aligned}$$

In passing from the first to the second line we have applied the inequality $\ln(z) < z - 1$ for $z > 1$. From the second to the third line we have used $[1 - \tanh(\tilde{J}_q)] / \mathcal{A}_3(\tilde{J}_q) > 1$ for $1/(z-1) < \tanh(\tilde{J}_q) < 1/\sqrt{z-1}$. Finally, in the last line we used that $1 - \mathcal{A}_2(x_0, x_q) - \mathcal{A}_2(x_q, x_0) = 0$, which follows by simply writing out the terms.

Combining the results we find that $\mathcal{A}_1(\tilde{J}_0, \tilde{J}_q) > 0$ for $\tilde{J}_c^{\text{BG}} < \tilde{J}_q < \tilde{J}_0$, and therefore $t_c^{\text{BG}}(\tilde{J}_0, \tilde{J}_q)$ is bounded by Eq. (S21) in this regime.

S5. RELAXATION DYNAMICS

In this section we focus on the relaxation dynamics of the minima of the rate function, $\tilde{m}(t, \tilde{J}_0, \tilde{J}_q) \equiv \arg \min_m V(m, \tilde{J}_q, t)$. Based on the first characteristic equation in Eq. (S1) we find that the minima obey the differential equation

$$\frac{d\tilde{m}(t, \tilde{J}_0, \tilde{J}_q)}{dt} = 2w^+(\tilde{m}, \tilde{J}_q) - 2w^-(\tilde{m}, \tilde{J}_q). \quad (\text{S25})$$

As the right-hand side (RHS) does not depend explicitly on time, the solution is given by the integral

$$\frac{1}{2} \int \frac{d\tilde{m}}{w^+(\tilde{m}, \tilde{J}_q) - w^-(\tilde{m}, \tilde{J}_q)} = t + \mathcal{C}, \quad (\text{S26})$$

where $\mathcal{C} = \mathcal{C}(\tilde{J}_0, \tilde{J}_q)$ is an integration constant left to be determined from the initial condition at $t = 0$. The integral on the left-hand side (LHS) cannot be evaluated analytically upon inserting the MF transition rates (see Eq. (3) in [1] for their functional form). However, for the BG transition rates given by Eq. (4) in the Letter, the integral can be evaluated explicitly for $\bar{z} = \{2, 3, 4, 5, 6\}$. Here we show the analysis for $\bar{z} = \{2, 4\}$, where we use the former as an educative introduction to carry out the latter. Our aim is to go beyond the linear response regime studied in [6] by applying the so-called *Lagrange Inversion Theorem*.

A. BG approximation with $\bar{z} = 2$

Formally the mean magnetization for $\bar{z} = 2$ vanishes for any initial and final temperature. However, instead of considering a temperature quench, we consider a magnetization quench where we initially prepare the system in a non-zero magnetic state with $\tilde{m}(0) \equiv \tilde{m}_0 \neq 0$. Inserting the BG transition rates with $\bar{z} = 2$ into Eq. (S26) we obtain – after some algebraic manipulation – the result

$$- \tau_r(\tilde{J}_q) \ln(\tilde{m}/g(\tilde{m}, \tilde{J}_q)) = t + \mathcal{C}, \quad (\text{S27})$$

where $1/\tau_r(\tilde{J}_q) \equiv 4w_{\text{BG}}^\pm(0, \tilde{J}_q)\tilde{f}_{\text{BG}}''(0, \tilde{J}_q) = 8/(1 + e^{2\tilde{J}_q})^2$ is the relaxation rate for $\bar{z} = 2$, and we have introduced the auxiliary function

$$g(\tilde{m}, \tilde{J}_q) \equiv \exp(-\tanh(\tilde{J}_q) \ln(\alpha_+) - \alpha_- / (2 \cosh(\tilde{J}_q) \tilde{m}^2)), \quad (\text{S28})$$

with

$$\alpha_\pm(\tilde{m}, \tilde{J}_q) \equiv \exp(2\tilde{J}_q) \pm [\tilde{m}^2 + \exp(4\tilde{J}_q)(1 - \tilde{m}^2)]^{1/2}. \quad (\text{S29})$$

From Eq. (S27) we directly read off the integration constant $\mathcal{C} = \mathcal{C}(\bar{m}_0, \tilde{J}_q)$ at $t = 0$. To obtain an explicit solution for \bar{m} we multiply both sides of Eq. (S27) by $-\tau_r$, and subsequently exponentiate, resulting in

$$\frac{\bar{m}}{g(\bar{m}, \tilde{J}_q)} = \frac{\bar{m}_0}{g(\bar{m}_0, \tilde{J}_q)} e^{-t/\tau_r(\tilde{J}_q)}, \quad (\text{S30})$$

where we have now also fixed the integration constant. Now we invoke the *Lagrange inversion theorem*: Let $f(w)$ be analytic in some neighborhood of the point $w = 0$ (of the complex plane) with $f(0) \neq 0$ and let it satisfy the equation

$$\frac{w}{f(w)} = \xi. \quad (\text{S31})$$

Then $\exists a, b \in \mathbb{R}^+$ such that for $|\xi| < a$ Eq. (S31) has only a single solution in the domain $|w| < b$. According to the Lagrange-Bürmann formula this unique solution is an analytical function of ξ given by

$$w = \sum_{k=1}^{\infty} \frac{\xi^k}{k!} \left[\frac{d^{k-1}}{dw^{k-1}} f(w)^k \right]_{w=0}. \quad (\text{S32})$$

Note that Eq. (S30) is similar in structure to Eq. (S31), and furthermore

$$g(0, \tilde{J}_q) = \exp(-\tanh(\tilde{J}_q)(1/2 + \ln 2 + 2\tilde{J}_q)), \quad (\text{S33})$$

which is non-zero $\forall \tilde{J}_q \in \mathbb{R}$. Therefore, we can use Eq. (S32) to obtain an explicit solution for \bar{m} , yielding

$$\bar{m}(t, \bar{m}_0, \tilde{J}_q) = \sum_{k=1}^{\infty} \frac{\bar{m}_0^k}{g(\bar{m}_0, \tilde{J}_q)^k k!} \left[\frac{d^{k-1}}{dw^{k-1}} g(\bar{m}, \tilde{J}_q)^k \right]_{\bar{m}=0} e^{-kt/\tau_r(\tilde{J}_q)} = \sum_{k=1}^{\infty} \alpha_k(\bar{m}_0, \tilde{J}_q) e^{-kt/\tau_r(\tilde{J}_q)}. \quad (\text{S34})$$

For completeness, we list the first three non-zero coefficients

$$\begin{aligned} \alpha_1(\bar{m}_0, \tilde{J}_q) &= \bar{m}_0 g(0, \tilde{J}_q) / g(\bar{m}_0, \tilde{J}_q), \\ \alpha_3(\bar{m}_0, \tilde{J}_q) &= \alpha_1^3(\bar{m}_0, \tilde{J}_q) e^{-4\tilde{J}_q} (1 - e^{2\tilde{J}_q})^2 / 8, \\ \alpha_5(\bar{m}_0, \tilde{J}_q) &= \alpha_1^5(\bar{m}_0, \tilde{J}_q) e^{-4\tilde{J}_q} \sinh(\tilde{J}_q)^3 (4 \cosh(\tilde{J}_q) + 5 \sinh(\tilde{J}_q)) / 8. \end{aligned} \quad (\text{S35})$$

Note that $\alpha_1(\bar{m}_0, 0) = \bar{m}_0$ and $\alpha_k(\bar{m}_0, 0) = 0 \forall k \in \{2, 3, \dots\}$, which gives the well-known result $\bar{m}(t, \bar{m}_0, 0) = \bar{m}_0 \exp(-2t)$ [4]. Furthermore, since $g(\bar{m}, \tilde{J}_q) = g(-\bar{m}, \tilde{J}_q)$, we know that $\alpha_{2k} = 0 \forall k \in \mathbb{N}$. This concludes our derivation of $\bar{m}(t, \bar{m}_0, \tilde{J}_q)$ for $\bar{z} = 2$.

B. BG approximation with $\bar{z} = 4$

Now we focus on the case $\bar{z} = 4$. The analysis requires the same steps as shown in the previous section, but involves a bit more algebra. We will focus only on quenches where the initial temperature is below the critical temperature, i.e. $\tilde{J}_0 > \tilde{J}_c^{\text{BG}} = \ln(2)/2$, resulting in the following initial magnetization [7]

$$\bar{m}_0(\tilde{J}_0) = e^{2\tilde{J}_0} (e^{4\tilde{J}_0} - 4)^{1/2} / (e^{4\tilde{J}_0} - 2). \quad (\text{S36})$$

In order to apply the *Lagrange inversion theorem* we have to make a distinction between quenches above and below the critical temperature, since they have different equilibrium states. Furthermore, for quenches above the critical temperature $\tilde{J}_q \leq \ln(2)/2$, we will encounter a particular ‘‘special’’ value $\tilde{J}_q = \ln(2)/4$ which needs to be handled separately.

1. $\tilde{J}_q < \ln(2)/2$ and $\tilde{J}_q \neq \ln(2)/4$

Upon determining the integral in Eq. (S26) for $\bar{z} = 4$ we obtain an analytic expression which can be written in a similar form as Eq. (S27). In this regime the relaxation rate is given by

$1/\tau_r(\tilde{J}_q) \equiv 4w_{\text{BG}}^{\pm}(\tilde{J}_q)\tilde{f}_{\text{BG}}''(0, \tilde{J}_q) = \cosh^4(\tilde{J}_q)/(4\exp(-2\tilde{J}) - 2)$, which is plotted in Fig. 2f in the main Letter (blue line, left side of black dashed line). The auxiliary function $g(\tilde{m}, \tilde{J}_q)$ in Eq. (S27) is now given by

$$g(\tilde{m}, \tilde{J}_q) = \prod_{i=1}^5 g_i(\tilde{m}, \tilde{J}_q), \quad (\text{S37})$$

which we have further divided into sub-auxiliary functions that read

$$\begin{aligned} g_1(\tilde{m}, \tilde{J}_q) &= \exp\left(\frac{\alpha_- \operatorname{sech}(\tilde{J}_q)^6 (1 - 3 \tanh(\tilde{J}_q))(2 + e^{2\tilde{J}_q})^2}{8m^4(\tanh(\tilde{J}_q) - 3)^3}\right), \\ g_2(\tilde{m}, \tilde{J}_q) &= \exp\left(\frac{e^{2\tilde{J}_q}(2 - e^{2\tilde{J}_q})(2\alpha_- + (13\alpha_- - 2)e^{2\tilde{J}_q} + (5\alpha_- + 1)e^{4\tilde{J}_q} + e^{6\tilde{J}_q})}{(1 + e^{2\tilde{J}_q})^3(2 + e^{2\tilde{J}_q})^2 m^2}\right), \\ g_3(\tilde{m}, \tilde{J}_q) &= \alpha_+(\tilde{m}, \tilde{J}_q)^{\nu_1(\tilde{J}_q)}, \\ g_4(\tilde{m}, \tilde{J}_q) &= [4\tilde{m}^2 - e^{4\tilde{J}_q}(e^{4\tilde{J}_q} - 4)(1 - \tilde{m}^2)]^{\nu_2(\tilde{J}_q)}, \\ g_5(\tilde{m}, \tilde{J}_q) &= [4\tilde{m}^2 + e^{4\tilde{J}_q}((2 - \alpha_+ + e^{2\tilde{J}_q} - e^{4\tilde{J}_q})^2 - \tilde{m}^2(3 - e^{4\tilde{J}_q})^2)]^{-\nu_2(\tilde{J}_q)/2}, \end{aligned} \quad (\text{S38})$$

and $\alpha_{\pm}(\tilde{m}, \tilde{J}_q)$ is given by Eq. (S29). The exponents in the last three equations are given by

$$\begin{aligned} \nu_1(\tilde{J}_q) &\equiv [44 \tanh(\tilde{J}_q) - 20 + \operatorname{sech}(\tilde{J}_q)^4(3 \tanh(\tilde{J}_q) - 1) + \operatorname{sech}(\tilde{J}_q)^2(19 \tanh(\tilde{J}_q) - 11)](\tanh(\tilde{J}_q) - 3)^{-3}, \\ \nu_2(\tilde{J}_q) &\equiv 32e^{2\tilde{J}_q}(2 + e^{2\tilde{J}_q})^{-3}(e^{4\tilde{J}_q} - 2)^{-1}. \end{aligned} \quad (\text{S39})$$

Note that $\nu_1 \rightarrow \infty$ for $\tilde{J}_q \rightarrow \ln(2)/2$ and $\nu_2 \rightarrow \infty$ for $\tilde{J}_q \rightarrow \ln(2)/4 < \ln(2)/2$. The latter value is a particular point where the integral Eq. (S26) drastically simplifies as we will see in the next section. To check whether we can apply the *Lagrange inversion theorem* we first need to determine $g(0, \tilde{J}_q)$, which results in

$$g(0, \tilde{J}_q) = 2^{\nu_1(\tilde{J}_q) - \nu_2(\tilde{J}_q)} \exp(2[\nu_1(\tilde{J}_q) + \nu_2(\tilde{J}_q)]\tilde{J}_q - \nu_3(\tilde{J}_q)) |\coth(\tilde{J}_q) - 3|^{\nu_2(\tilde{J}_q)}, \quad (\text{S40})$$

where we have defined the auxiliary function

$$\nu_3(\tilde{J}_q) = (9e^{8\tilde{J}_q} - 2e^{6\tilde{J}_q} - 51e^{4\tilde{J}_q} + 32e^{2\tilde{J}_q} + 12)/4(e^{4\tilde{J}_q} + 3e^{2\tilde{J}_q} + 2)^2. \quad (\text{S41})$$

For $\tilde{J}_q < \ln(2)/2$ and $\tilde{J}_q \neq \ln(2)/4$ we have $\coth(\tilde{J}_q) - 3 \neq 0$ and $|\nu_{1,2,3}(\tilde{J}_q)| < \infty$. Hence, in this regime $g(0, \tilde{J}_q) \neq 0$, and therefore we can use the *Lagrange inversion theorem* as in the previous section. Plugging $g(\tilde{m}, \tilde{J}_q)$ given by Eq. (S37) into Eq. (S34), and using Eq. (S36) to express \tilde{m}_0 in terms of \tilde{J}_0 , we obtain the power series solution as mentioned in the main Letter. For completeness, we list the first three non-zero coefficients

$$\begin{aligned} \alpha_1(\tilde{J}_0, \tilde{J}_q) &= \tilde{m}_0 g(0, \tilde{J}_q) / g(\tilde{m}_0, \tilde{J}_q), \\ \alpha_3(\tilde{J}_0, \tilde{J}_q) &= \alpha_1^3(\tilde{J}_0, \tilde{J}_q) e^{-4\tilde{J}_q} (4 - e^{2\tilde{J}_q}) (1 - e^{2\tilde{J}_q})^2 / (4(2 - e^{2\tilde{J}_q})), \\ \alpha_5(\tilde{J}_0, \tilde{J}_q) &= \alpha_1^5(\tilde{J}_0, \tilde{J}_q) \frac{111 \cosh(\tilde{J}_q) - 87 \cosh(3\tilde{J}_q) - 313 \sinh(\tilde{J}_q) + 113 \sinh(3\tilde{J}_q)}{8(\coth(\tilde{J}_q) - 3)^2} e^{-4\tilde{J}_q} \sinh(\tilde{J}_q). \end{aligned} \quad (\text{S42})$$

Note that only terms of \tilde{m}^2 and \tilde{m}^4 enter in $g(\tilde{m}, \tilde{J}_q)$ given by Eq. (S37). Therefore $g(\tilde{m}, \tilde{J}_q) = g(-\tilde{m}, \tilde{J}_q)$, which implies that $\alpha_{2k} = 0 \forall k \in \mathbb{N}$. Furthermore, we also have $\alpha_1(\tilde{J}_0, 0) = 1$ and $\alpha_k(\tilde{J}_0, 0) = 0 \forall k \in \{2, 3, \dots\}$ as in the previous section. The first two coefficients $\alpha_{1,3}$ are displayed in the inset of Fig. 2d in the Letter.

2. $\tilde{J}_q = \ln(2)/4$

For $\tilde{J}_q = \ln(2)/4$ the outcome of the integral in Eq. (S27) simplifies drastically, and the resulting expression for the auxiliary function $g(\tilde{m}, \ln(2)/4)$ reads

$$g(m, \ln(2)/4) = \exp\left(\frac{c_1 + c_2 m^2 - (c_1 + (c_1/4 + c_2)\tilde{m}^2 - \sqrt{2}c_3\tilde{m}^4)[1 - \tilde{m}^2/2]^{1/2}}{m^4}\right) (2 + [4 - 2m^2]^{1/2})^{c_4}, \quad (\text{S43})$$

with the numerical coefficients given by

$$c_1 = 560\sqrt{2} - 792, \quad c_2 = 1092 - 772\sqrt{2}, \quad c_3 = 8(7 - 5\sqrt{2}), \quad c_4 = 329 - 232\sqrt{2}. \quad (\text{S44})$$

This function attains the following value at $\bar{m} = 0$

$$g(0, \ln(2)/4) = 4^{c_4} \exp\left(\frac{3c_1}{32} + \frac{c_2}{4} + \sqrt{2}c_3\right). \quad (\text{S45})$$

Hence, $g(0, \ln(2)/4) \neq 0$, and therefore we can use the *Lagrange inversion theorem*. Inserting Eq. (S43) into Eq. (S34) we obtain an expression for the coefficients. The result for the first three non-zero coefficients reads

$$\begin{aligned} \alpha_1(\tilde{J}_0, \ln(2)/4) &= \bar{m}_0 g(0, \ln(2)/4) / g(\bar{m}_0, \ln(2)/4), \\ \alpha_3(\tilde{J}_0, \ln(2)/4) &= \alpha_1^3(\tilde{J}_0, \ln(2)/4) (c_1 + 2c_2 - 8(2\sqrt{2}c_3 + c_4)) / 4^3, \\ \alpha_5(\tilde{J}_0, \ln(2)/4) &= \alpha_1^5(\tilde{J}_0, \ln(2)/4) \mathcal{A}(c_1, c_2, c_3, c_4) / 2^{13}, \end{aligned} \quad (\text{S46})$$

with

$\mathcal{A}(c_1, c_2, c_3, c_4) = 5c_1^2 + 20c_2^2 + 4c_1(9 + 5c_2 - 40\sqrt{2}c_3 - 20c_4) + 32c_2(2 - 10\sqrt{2}c_3 - 5c_4) + 64(40c_3^2 + c_4(5c_4 - 3) + 4\sqrt{2}c_3(5c_4 - 1))$. Also here we find that only terms of \bar{m}^2 and \bar{m}^4 enter in Eq. (S43), which implies that $\alpha_{2k} = 0 \forall k \in \mathbb{N}$. Notably, the coefficients in Eq. (S42) approach Eq. (S46) in the neighborhood of $\tilde{J}_q = \ln(2)/4$.

3. $\tilde{J}_q > \ln(2)/2$

Finally, we focus on a quench in the two-phase domain with $\tilde{J}_q > \ln(2)/2$. Formally the integral given by Eq. (S26) does not change w.r.t. the analysis for $\tilde{J}_q < \ln(2)/2$. However, there is a difference in applying the *Lagrange inversion theorem*, since the steady-state magnetization $\bar{m}_\infty(\tilde{J}_q) = \pm e^{2\tilde{J}_q} (e^{4\tilde{J}_q} - 4)^{1/2} / (e^{4\tilde{J}_q} - 2)$ maintains a non-zero value for $\tilde{J}_q > \ln(2)/2$. The relaxation rate now reads

$1/\tau_r(\tilde{J}_q) = 4w_{\text{BG}}^\pm(m_\infty, \tilde{J}_q) \tilde{f}_{\text{BG}}''(\bar{m}_\infty, \tilde{J}_q) = (e^{4\tilde{J}_q} - 2)(e^{2\tilde{J}_q} - 2)(e^{2\tilde{J}_q} + 2)^3 / (e^{4\tilde{J}_q} + 1)^4$ (see blue line in Fig. 2f on right side of black dashed line). After some algebraic manipulation, we obtain

$$- \tau_r(\tilde{J}_q) \ln\left(\frac{\bar{m} - \bar{m}_\infty}{g(\bar{m}, \tilde{J}_q)}\right) = t + \mathcal{C}, \quad (\text{S47})$$

where $\mathcal{C} = \mathcal{C}(\tilde{J}_0, \tilde{J}_q)$ is the integration constant determined by the initial condition. The function $g(\bar{m}, \tilde{J}_q)$ reads

$$g(\bar{m}, \tilde{J}_q) = (e^{4\tilde{J}_q} - 2)^{-1} \prod_{i=1}^5 g_i(\bar{m}, \tilde{J}_q), \quad (\text{S48})$$

which we have further divided into the following sub-auxiliary functions

$$\begin{aligned} g_1(\bar{m}, \tilde{J}_q) &= \exp\left(\frac{\alpha_-(e^{4\tilde{J}_q} - 2)(e^{2\tilde{J}_q} + 2)^2(2 - e^{2\tilde{J}_q})e^{4\tilde{J}_q}}{16m^4(1 + e^{2\tilde{J}_q})^4}\right), \\ g_2(\bar{m}, \tilde{J}_q) &= \exp\left(\frac{e^{4\tilde{J}_q}(8 - 6e^{4\tilde{J}_q} + e^{8\tilde{J}_q})(14 + 20e^{2\tilde{J}_q} + 6e^{4\tilde{J}_q} - e^{-4\tilde{J}_q}(e^{2\tilde{J}_q} + 1)(2 + 13e^{2\tilde{J}_q} + 5e^{4\tilde{J}_q})(\alpha_+ - e^{2\tilde{J}_q}))}{32(1 + e^{2\tilde{J}_q})^4 m^2}\right), \\ g_3(\bar{m}, \tilde{J}_q) &= [\bar{m}^2(e^{4\tilde{J}_q} - 2)^2(1 - e^{4\tilde{J}_q}) + 4e^{4\tilde{J}_q}(1 - \alpha_+ + e^{2\tilde{J}_q}) - e^{8\tilde{J}_q}(3 - 2\alpha_+ + 2e^{2\tilde{J}_q}) + e^{12\tilde{J}_q}]^{1/2}, \\ g_4(\bar{m}, \tilde{J}_q) &= |\bar{m}(e^{4\tilde{J}_q} - 2) + e^{2\tilde{J}_q}(e^{4\tilde{J}_q} - 4)^{1/2}|^{-1}, \\ g_5(\bar{m}, \tilde{J}_q) &= \bar{m}^{\nu_1(\tilde{J}_q)}, \\ g_6(\bar{m}, \tilde{J}_q) &= \alpha_+^{-\nu_2(\tilde{J}_q)}. \end{aligned} \quad (\text{S49})$$

The function $\alpha_\pm(\bar{m}, \tilde{J}_q)$ is given by Eq. (S29), and the exponents in the last two equations are given by

$$\begin{aligned} \nu_1(\tilde{J}_q) &\equiv e^{-2\tilde{J}_q}(e^{2\tilde{J}_q} + 2)^3(e^{4\tilde{J}_q} - 2)/32, \\ \nu_2(\tilde{J}_q) &\equiv e^{\tilde{J}_q}(e^{4\tilde{J}_q} - 2) \operatorname{sech}(\tilde{J}_q)(28 + 31 \cosh(2\tilde{J}_q) + 5 \cosh(4\tilde{J}_q) - 41 \sinh(2\tilde{J}_q) - 11 \sinh(4\tilde{J}_q) - 6 \tanh(\tilde{J}_q))/64. \end{aligned} \quad (\text{S50})$$

In order to apply the *Lagrange inversion theorem* we need to evaluate $g(\bar{m}, \tilde{J}_q)$ at the steady state \bar{m}_∞ , which yields

$$g(\bar{m}_\infty, \tilde{J}_q) = (\bar{m}_\infty)^{\nu_1(\tilde{J}_q)} (1 + e^{2\tilde{J}_q} + 2(e^{4\tilde{J}_q} - 2)^{-1})^{-\nu_2(\tilde{J}_q)} e^{2\tilde{J}_q - \nu_3(\tilde{J}_q)} (e^{4\tilde{J}_q} - 2)^{-1/2}, \quad (\text{S51})$$

where we have defined the auxiliary function

$$\nu_3(\tilde{J}_q) = e^{3\tilde{J}_q} (13 + 8 \cosh(2\tilde{J}_q)) (\cosh(\tilde{J}_q) - 3 \sinh(\tilde{J}_q)) (\cosh(\tilde{J}_q) - \sinh(\tilde{J}_q) (6 - \tanh(\tilde{J}_q)))^2. \quad (\text{S52})$$

For $\tilde{J}_q > \ln(2)/2$ we find that $g(\bar{m}_\infty, \tilde{J}_q) \neq 0$, and therefore we can apply the *Lagrange inversion theorem*. Upon inverting Eq. (S47), the final result reads

$$\begin{aligned} \bar{m}(t, \bar{m}_0, \tilde{J}_q) &= \bar{m}_\infty + \sum_{k=1}^{\infty} \frac{(\bar{m}_0 - \bar{m}_\infty)^k}{g(\bar{m}_0, \tilde{J}_q)^k k!} \left[\frac{d^{k-1}}{dw^{k-1}} g(\bar{m}, \tilde{J}_q)^k \right]_{\bar{m}=\bar{m}_\infty} e^{-kt/\tau_r(\tilde{J}_q)} \\ &= \bar{m}_\infty + \sum_{k=1}^{\infty} \alpha_k(\tilde{J}_0, \tilde{J}_q) e^{-kt/\tau_r(\tilde{J}_q)}. \end{aligned} \quad (\text{S53})$$

For completeness, we list the first three non-zero coefficients

$$\begin{aligned} \alpha_1(\tilde{J}_0, \tilde{J}_q) &= (\bar{m}_0 - \bar{m}_\infty) g(\bar{m}_\infty, \tilde{J}_q) / g(\bar{m}_0, \tilde{J}_q), \\ \alpha_2(\tilde{J}_0, \tilde{J}_q) &= \alpha_1^2(\tilde{J}_0, \tilde{J}_q) e^{-6\tilde{J}_q} (e^{4\tilde{J}_q} - 2)^2 (4e^{3\tilde{J}_q} \sinh(\tilde{J}_q) - 1) / (e^{4\tilde{J}_q} - 4)^{1/2}, \\ \alpha_3(\tilde{J}_0, \tilde{J}_q) &= \alpha_1^3(\tilde{J}_0, \tilde{J}_q) e^{-6\tilde{J}_q} (e^{4\tilde{J}_q} - 2)^3 (52 - 10e^{-6\tilde{J}_q} - 24e^{-4\tilde{J}_q} + 25e^{-2\tilde{J}_q} - 35e^{2\tilde{J}_q} - 18e^{4\tilde{J}_q} + 11e^{6\tilde{J}_q}) / 2(e^{4\tilde{J}_q} - 4). \end{aligned} \quad (\text{S54})$$

The inset of Fig. 2e in the main Letter displays the first two coefficients $\alpha_{1,2}$. This concludes our derivation for the relaxation dynamics of the rate function minima.

S6. RELATIVE ENTROPY

Here we derive the coefficients γ_k for the power series expansion of the relative entropy per spin, given by Eq. (10) in the Letter. The relative entropy is evaluated with the saddle point approximation in the thermodynamic limit, which results in

$$\mathcal{D}_t = \lim_{N \rightarrow \infty} \int_{-1}^1 e^{-NV(m, \tilde{J}_q, t)} [V_{\text{eq}}(m, \tilde{J}_q) - V(m, \tilde{J}_q, t)] dm \simeq V_{\text{eq}}(\bar{m}(t, \tilde{J}_0, \tilde{J}_q), \tilde{J}_q) = \sum_{k=2}^{\infty} \gamma_k(\tilde{J}_0, \tilde{J}_q) e^{-kt/\tau_r(\tilde{J}_q)}. \quad (\text{S55})$$

To arrive at the second equality we have applied the saddle point approximation around the minimum $\bar{m}(t, \tilde{J}_0, \tilde{J}_q)$ of the rate function $V(m, \tilde{J}_q, t)$ at time t . Note that $V(\bar{m}, \tilde{J}_q, t) = 0$, and therefore only the equilibrium potential $V_{\text{eq}}(\bar{m}, \tilde{J}_q)$ remains after the saddle point approximation. For the final equality we carried out a Taylor expansion around the steady state \bar{m}_∞ , and used the power series expansion of $\bar{m}(t, \tilde{J}_0, \tilde{J}_q)$ which is analyzed in Sec. S5. The first three non-zero coefficients in Eq. (S55) are given by

$$\begin{aligned} \gamma_2(\tilde{J}_0, \tilde{J}_q) &= \alpha_1^2 V_{\text{eq}}''(\bar{m}_\infty, \tilde{J}_q) / 2, \\ \gamma_3(\tilde{J}_0, \tilde{J}_q) &= \alpha_1 \alpha_2 V_{\text{eq}}''(\bar{m}_\infty, \tilde{J}_q) + \alpha_1^3 V_{\text{eq}}'''(\bar{m}_\infty, \tilde{J}_q) / 6, \\ \gamma_4(\tilde{J}_0, \tilde{J}_q) &= (\alpha_2^2 / 2 + \alpha_1 \alpha_3) V_{\text{eq}}''(\bar{m}_\infty, \tilde{J}_q) + \alpha_1^2 \alpha_2 V_{\text{eq}}'''(\bar{m}_\infty, \tilde{J}_q) / 2 + \alpha_1^4 V_{\text{eq}}''''(\bar{m}_\infty, \tilde{J}_q) / 24, \end{aligned} \quad (\text{S56})$$

where the coefficients $\alpha_i = \alpha_i(\tilde{J}_0, \tilde{J}_q)$ are given by Eq. (S42) and (S54) for quenches in the one- and two-phase domain. For quenches in the one-phase domain we have $\gamma_3(\tilde{J}_0, \tilde{J}_q) = 0$ since $\bar{m}_\infty = 0$ and $\alpha_2 = V_{\text{eq}}'''(0, \tilde{J}_q) = 0$. The inset of Fig. 3a in the Letter displays the first two non-zero coefficients for quenches in the one- and two-phase domain.

S7. PARITY SYMMETRY FOR THE STAGGERED MAGNETIZATION

Let us define the staggered magnetization $\hat{m} \in [-1, 1]$ in the Ising model as

$$\hat{m} \equiv N^{-1} \sum_{i=1}^N (-\sigma_i)^i. \quad (\text{S57})$$

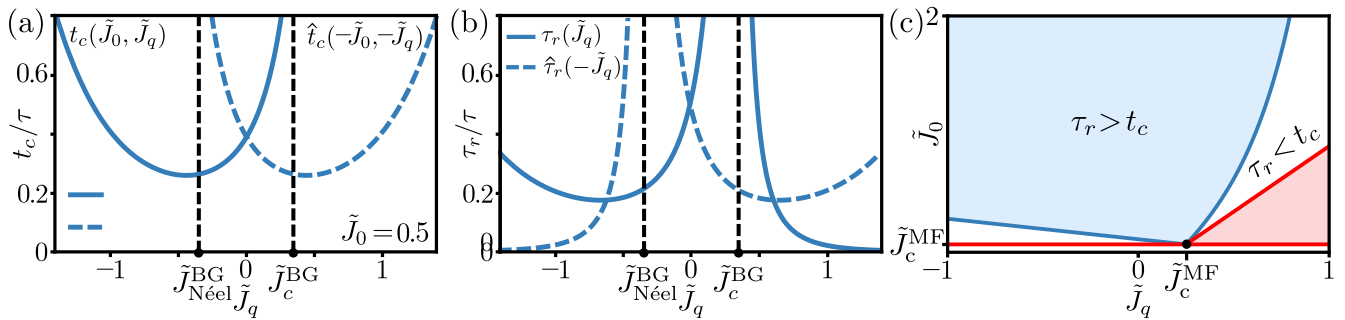


FIG. S3. **Parity symmetry for the staggered magnetization and the MF dynamical phase diagram.** In all panels we consider a lattice with $\bar{z} = 4$. (a)-(b) Critical time (a) and relaxation time (b) as a function of the quench temperature \tilde{J}_q . The dashed lines correspond to the staggered magnetization dynamics, for which a parity symmetry applies w.r.t. the temperature $\tilde{J} \rightarrow -\tilde{J}$ (see Eq. (S58)). (c) Dynamical phase diagram for the MF critical time t_c^{MF} and relaxation τ_r^{MF} time. The red area is forbidden since $\tilde{J}_0 > \tilde{J}_q$. Inside the blue area, the relaxation time is larger than the critical time. The dark blue phase boundary where $t_c^{\text{MF}} = \tau_r^{\text{MF}}$ is given by Eq. (S61). The MF critical point reads $\tilde{J}_c^{\text{MF}} \equiv 1/\bar{z}$. Fig. 3b in the main Letter shows the BG dynamical phase diagram.

For perfectly anti-ferromagnetic order we have $\hat{m} = \pm 1$, and for anti-ferromagnetic disorder $\hat{m} = 0$. Based on the works in [8–10] we know that the BG free energy density $\tilde{f}_{\text{BG}}(m, \tilde{J})$ obeys the following parity symmetry w.r.t. the staggered magnetization

$$\tilde{f}_{\text{BG}}(m, \tilde{J}) = \tilde{f}_{\text{BG}}(\hat{m}, -\tilde{J}). \quad (\text{S58})$$

Therefore, our results for the critical time, relaxation time, and dynamical phase diagram also apply for dynamics of staggered magnetization upon inverting the temperature $\tilde{J} \rightarrow -\tilde{J}$. In Fig. S3a-b we depict the critical time \hat{t}_c (a) and relaxation time $\hat{\tau}_r$ (b) for the dynamics of the staggered magnetization with the blue dashed lines.

S8. MF DYNAMICAL PHASE DIAGRAM

Fig. S3c depicts the MF dynamical phase diagram. To obtain the blue shaded area where $\tau_r^{\text{MF}} > t_c^{\text{MF}}$, we first compute the MF critical time. Inserting the MF transition rates and free energy density into Eq. (7) in the main letter we obtain the MF critical time

$$t_c^{\text{MF}}(\tilde{J}_0, \tilde{J}_q) = \frac{1}{4(1 - \bar{z}\tilde{J}_q)} \ln \left(\frac{\bar{z}\tilde{J}_q - \bar{z}\tilde{J}_0}{1 - \bar{z}\tilde{J}_0} \right), \quad (\text{S59})$$

which is also reported in [1, 3, 4] for $\bar{z} = 1$. The MF relaxation time is given by $\tau_r^{\text{MF}}(\tilde{J}_q) \equiv 1/4w_{\text{MF}}^{\pm}(\bar{m}, \tilde{J}_q)\tilde{f}_{\text{MF}}''(\bar{m}, \tilde{J}_q)$, where $\bar{m} = \arg \min_m \tilde{f}_{\text{MF}}(m, \tilde{J}_q)$ is given by the transcendental equation

$$\bar{m} = \tanh(\bar{z}\tilde{J}_q\bar{m}). \quad (\text{S60})$$

Equating t_c^{MF} and τ_r^{MF} we obtain the dark blue boundary line

$$\bar{z}\tilde{J}_0^{\dagger} = \frac{\bar{z}\tilde{J}_q \exp \left(\frac{2(1+\bar{m})(\bar{z}\tilde{J}_q-1)}{1-(1-\bar{m}^2)\bar{z}\tilde{J}_q} e^{-\bar{z}\bar{m}\tilde{J}_q} \right) - 1}{\exp \left(\frac{2(1+\bar{m})(\bar{z}\tilde{J}_q-1)}{1-(1-\bar{m}^2)\bar{z}\tilde{J}_q} e^{-\bar{z}\bar{m}\tilde{J}_q} \right) - 1}. \quad (\text{S61})$$

For $\tilde{J}_0 > \tilde{J}_0^{\dagger}$ (blue region) the MF relaxation time is larger than the critical time, i.e. $\tau_r^{\text{MF}} > t_c^{\text{MF}}$. For $1/\bar{z} < \tilde{J}_0 < \tilde{J}_0^{\dagger}$ (white region) the MF critical time is larger than the relaxation time.

[1] J. Meibohm and M. Esposito, *Phys. Rev. Lett.* **128**, 110603 (2022).

[2] J. Meibohm and M. Esposito, arXiv preprint arXiv:2205.10311 (2022).

- [3] C. Külske and A. Le Ny, *Commun. Math. Phys.* **271**, 431–454 (2007).
- [4] V. Ermolaev and C. Külske, *J. Stat. Phys.* **141**, 727–756 (2010).
- [5] E. R. Love, *The Mathematical Gazette* **64**, 55 (1980).
- [6] Y. Saito and R. Kubo, *J. Stat. Phys.* **15**, 233 (1976).
- [7] K. Blom and A. Godec, *Phys. Rev. X* **11**, 031067 (2021).
- [8] S. Katsura and M. Takizawa, *Prog. Theor. Exp. Phys.* **51**, 82 (1974).
- [9] I. Ono, *J. Phys. C Solid State Phys.* **17**, 3615 (1984).
- [10] F. Peruggi, F. di Liberto, and G. Monroy, *J. Phys. A: Math. Gen.* **16**, 811 (1983).